REPUBLIC OF IRAQ

MINISTRYOF HIGHER EDUCATION AND SCINTIFIC RESEARCH

AL-FURAT AL-AWSAT TECHNICAL UNIVERSITY

ENGINEERING TECHNICAL COLLEGE-NAJAF

INDOOR MIMO – OPTICAL SYSTEM USING LASER DIODES ANGLE DIVERSITY RECEIVER WITH OFDM TECHNIQUE

Halla Kadhem Mohammad

M.Sc. Communication Techniques Eng.

2021

INDOOR MIMO – OPTICAL SYSTEM USING LASER DIODES ANGLE DIVERSITY RECEIVER WITH OFDM TECHNIQUE

THESIS

SUBMITTED TO COMMUNICATION DEPARTMENT

IN PARTIAL FULFILLMENT OF THE

REQUIREMENT OF THE DEGREE M.Sc.

BY

Halla Kadhem Mohammad

Supervised by

Dr. Nasir Hussein Selman

2021

Supervisor certification

I certify that this thesis "Indoor MIMO – Optical System Using Laser Diodes Angle Diversity Receiver with OFDM Technique" which being submitted by Halla Kadhem Mohammad was prepared under our supervision at Communication Department , technical college/ Najaf , Al- Furat Al-Awset Technical University As a partial of fulfillment of the requirement for degree of M. Sc.

Signature:

Name: **Dr. Nasir Hussein Selman**

Date: / /2022

In view of available recommendation, I forward this thesis for debate by the examining committee.

Signature:

Name :**prof.Dr. Ahmad T .Abdulsadda**

(Head of communication Tech. Eng. Dept.)

Date : / / 2022

Committee Report

We certify that we have read this thesis titled **"Indoor MIMO – Optical System Using Laser Diodes Angle Diversity Receiver with OFDM Technique"** which is being submitted by **Halla Kadhem Mohammad** and as examining Committee, examined the student in its contents. In our opinion, the thesis is adequate for award of degree of M.Sc.

Signature :

Name : **Dr. Nasir Hussein Selman**

Supervisor

Date : / / 2022

Signature :

Name : **Asst. Prof. Dr. Musa Hadi Wali**

(Member)

Date : / / 2022

Signature :

Name : **Dr.Salam Mahdi azooz**

(Member)

Date : / / 2022

Signature :

Name : **Prof. Dr. Saad Saffah Hassoon**

(chairman)

Date : / /2022

Approval of the technical college /Najaf

Signature :

Name : **Assistant Prof. Dr. Hassanain G. Hameed**

Dean of engineering technical college/Najaf

Date : / / 2022

Linguistic Certification

This is to certify that this thesis entitled “Indoor MIMO – Optical System Using Laser Diodes Angle Diversity Receiver with OFDM Technique” was reviewed linguistically. Its language was amended to meet the style of the English language.

Signature :

Name :

Date : / / 2021

Abstract

Visible Light Communications (VLC) is a promising and new technology for the next generation of wireless communication systems that use to improve the speed of data transmission. Moreover, a wireless optical networking technology that uses visible light as a data transmission medium to deliver high-speed communication in a communication system – like manner Wireless Fidelity (Wi-Fi).

This thesis presents a new algorithm for a Laser Diode (LD) positioning system based on ray tracing in the first-order reflection position. The system of VLC system uses laser diodes (LDs), each one consisting of 5 x 5 LD segments. A multipath propagation model and SNR evaluation are presented in this thesis.

In addition, a technology based on an 8×8 Multiple-Input Multiple-Output-Orthogonal Frequency Division Multiplexing (MIMO- OFDM) has been conducted. The real and imaginary sections of complex temporary OFDM signals are split in the work scheme, and these signals are subsequently sent across the MIMO-VLC channel utilizing indication modulation based on active LDs. Encoding complicated signal information into the location of the transmission LDs results in a higher spectrum and power efficiency. Furthermore, a maximum probability estimator is used to estimate those real and imaginary parts of OFDM signals at the receiver. Also, the Mean Squared Error (MSE) with respect to Signal to Noise ratio (SNR) was designed and simulated using MATLAB software.

Through the results obtained to the proposed system, it was found that the highest value of SNR was (50 dB) in the fourth position through sources (LD_1, LD_3) , and the

lowest value was (34dB) in the sixth position through sources (LD_2, LD_4). This is regarding the first part of this work (positioning and reflected algorithm).

As for optical MIMO-OFDM with LD index modulation, which is the second part of this work, it turns out that the highest value of SNR was (35 dB) when Bit Error Rate (BER) less than 10^{-2} that's about (0.0082) was in channel 5 at location (8,7) and the lowest value was (30 dB) when BER ($10^{-0.9}$) in channel 7 at location (8).

Finally, using analytic channel matrices, the MSE versus SNR curves for MIMO-OFDM are given. Theoretical values of small problems are compared with the results of computer simulations. It was found, the theoretical and computer simulation curves fit quite well particularly at high SNR levels.

Acknowledgment

First and foremost, Alhamdulillah for giving me the strength, patience, courage, and determination in completing this work. All grace and thanks belongs to **Almighty Allah**

I am pleased to extend my sincere thanks to my dear father and dear mother who have supervised and supported me throughout the process of writing this letter and my life in general.

I also express my thanks and gratitude to Dr. Nassir Hussein Salman for his supervision of this project, and also thanks and gratitude to Professor Dr. Faris Mohammed Ali for his guidance and support to complete this work. I also extend my sincere thanks to Dr. Ihsan Abdel Karim, my dear husband, for his guidance and suggestions to complete this work in its fullest form and for his continuous encouragement throughout the period of my studies.

I especially thank those of my dear brothers, friends and daughters who have stood by me and who have supported me spiritually.

DECLARATION

I hereby declare that the thesis is my original work except for quotations and citations which have been duly acknowledged.

2021 Halla Kadhem Mohammad

Contents

Title	page
Supervisor certification	ii
Committee Report	iii
Linguistic Certification	iv
Abstract	v
Acknowledgment	vii
Declaration	viii
Contents	ix
List of Tables	xii
List of Figures	xiii
Nomenclature	xvi
Abbreviations	xviii
Chapter One: Introduction	1
1.1 Overview of Visible Light Communication Systems (VLC)	1
1.2 Motivation:	4
1.3 Problem Statement	4
1.4 Thesis Objectives	5
1.5 Contributions	5
1.6 Scope of Work	6
1.7 Thesis Outline	7

Chapter Two: Literature Survey 8

2.1 Introduction of VLC Systems 8

2.2 VLC Applications 9

2.3 Indoor VLC System Structure 11

2.4 Comparison between Visible Light Communication and Radio Frequency 15

2.5 Literature Survey 19

Chapter Three: Methodology 28

3.1 Method Outline 28

3.2 Positioning and reflected algorithm 28

3.2.1 Laser VLC System and Room Setup 28

3.2.2 Calculations of received optical power 30

3.2.3 Line-of-Sight (LOS) analysis 31

3.2.4 First order reflection analysis 33

3.3 LD Index Modulation in Optical MIMO-OFDM 35

3.3.1 The Presence Of Frequency-Flat MIMO Channels with MIMO-OFDM 36

3.3.2 MIMO -OFDM with Conditional MAP Estimator 40

3.3.3 Calculation of Mean Square Error (MSE) 44

Chapter Four: Results and Discussions 47

4.1Result and Discussion 47

4.2 Laser VLC System and Room Setup 47

4.3 Generalized LD Index Modulation with Optical MIMO-OFDM 51

4.4 Analytical channel gain 52

4.5 Performance of MIMO –OFDM 54

Chapter Five: Conclusions and future work 58

5.1 Conclusion 58

5.2 Recommendations for future work 59

References 60

List Of Publication 68

List of Tables

Table	Page
Table 2.1: Comparison between Wi-Fi and Li-Fi systems in indoor wireless communications	17
Table 2.2: Comparison between laser diode (LD) and Light Emitting Diodes (LEDs)	18
Table 2.3 Summary of Literature Review	24
Table 3.1 Positioning VLC parameters	34
Table 3.2 MIMO-Optical VLC parameters	46
Table 4.1: PLOS & PFST in state of the position for blue color	48
Table 4.2: Show PLOS & PFST in state of the position for green color	49
Table 4.3: Show PLOS & PFST in state of the position for red color	50

List of Figures

Figure **Page**

Figure 1.1: Different light sources are compared in terms of luminous effectiveness. 3

Figure 1.2: RGB method 4

Figure 1.3: Block diagram of the scope of the work 6

Figure 2.1: Indoor VLC navigation system for visually impaired people. 10

Figure 2.2: Block diagram of VLC system 12

Figure 2.3: The two most common VLC connection configurations are (a) LOS transmission and (b) NLOS transmission 14

Figure 3.1 Room equipped with 5 laser diode sources with reflector 29

Figure 3.2 Ray tracing setup for LOS, first order reflections in VLC system 31

Figure 3.3 Ray tracing for LOS 32

Figure 3.4 Ray tracing for first order reflections 34

Figure 3.5 Block diagram of the MIMO -OFDM scheme for a 8 × 8 of VLC system 37

Figure 4.1: SNR versus POSITION using P_{LOS} & (P_{LOS} & P_{FST}) for blue color 48

Figure 4.2: SNR versus POSITION using P_{LOS} & (P_{LOS} & P_{FST}) for green color 49

Figure 4.3: SNR versus POSITION using P_{LOS} & (P_{LOS} & P_{FST}) for red color 50

Figure 4.5. Optical MIMO-OFDM performance BER comparison scheme in analytic channel H1 55

Figure 4.6. Optical MIMO-OFDM performance BER comparison scheme in analytic channel H2 55

Figure 4.7. Optical MIMO-OFDM performance BER comparison scheme in analytic channel H3 56

Figure 4.8. Optical MIMO-OFDM performance BER comparison scheme in analytic channel H4 56

Figure 4.9. Optical MIMO-OFDM performance BER comparison scheme in analytic channel H5 56

Figure 4.10. Optical MIMO-OFDM performance BER comparison scheme in analytic channel H6 56

Figure 4.11. Optical MIMO-OFDM performance BER comparison scheme in analytic channel H7 57

Figure 4.12. Optical MIMO-OFDM performance BER comparison scheme in analytic channel H8 57

Figure 4.13.Analytical and simulated MSE comparison for analytic channels 57

Nomenclature

Symbol	Definition
A	Detector area
DA_1	Area of the reflective element
M	Number of reflecting elements in the first order reflections
n	Mode number
n_t	Normal of the transmitter at location Rt
n_r	Normal of the receiver at the location Rr
P_S	Power source
P_r	Total received optical power
P_{LOS}	Power line of sight
P_{FST}	Power first order reflections
Rt	Location of transmitter
Rr	Location of receiver
R_d	Direct distance between the transmitter and the receiver
R_1	Distance between the transmitter and the reflected element
R_2	Distance between the reflected element and the receiver
S	Number of transmitter units

Greek Symbols	
α	Angle between the normal of the transmitter and the irradiance ray
δ	Angle of incidence with respect to the receiver normal
ψc	Concentrator's FOV (semi-angle)
β	the angle between the irradiance ray from the transmitter and the reflective element's normal
γ	is the angle between the reflective element's normal and the reflected ray toward the receiver
$\rho 1$	is the reflection coefficient of the reflective surface

Abbreviations

Symbol	Description
ACO	asymmetrically clipped optical
ADC	Analogue to Digital Convertor
BER	Bit Error Rate
BPF	Band Pass Filter
CCT	Correlated Colour Temperature
CDR	Call Detail Record
CP	Communication Plane
CSI	Channel State Information
DAC	Digital to Analogue Convertor
ERC	engineering research centre
FOV	Field Of View
FSO	Free Space Optical Communication
IFFT	Inverse Fast Fourier Transform
IrDA	Infrared Data Association
ISO	International Organization For Standardization
LD	Laser Diode
LEDs	Light Emitting Diodes
LOS	Line Of Sight
MAC	Medium Access Control
MAP	maximum a posteriori probability

MIMO	Multiple input multiple output
MSE	Mean Square Estimator
MUI	Material User Interface
NLOS	None Line Of Sight
NSF	National Science Foundation
OFDM	Orthogonal Frequency Division Multiplexing
OWC	Optical Wireless Communication
PD	Photo-detector
RF	Radio Frequency
RGB	Red-Green-Blue
SISO	Single Input Single Output
SNR	Signal-to-Noise Ratio
SSL	Solid State Lighting
TCA	Trans-conductance Amplifier
TIA	Trans-impedance Amplifier
VLC	Visible Light Communication

CHAPTER ONE

Introduction

1.1 Overview of Visible Light Communication Systems (VLC)

LiFi is an acronym for (Light Fidelity), which means ultra-high-definition and high-speed communication over visible light channels. It is also a secure, high-speed, bi-directional, and multi-user wireless network system that allows users to move around. As a result, it expands the range of VLC. Multiple Access Points (APs) are often required to create dense optical cellular networks in LiFi [1].

Traditional radio and microwave communication methods have limited channel bandwidth due to the limited radio spectrum accessible. Simultaneously, the data rates needed by users are increasing at an exponential rate. Many people nowadays carry many wireless gadgets with them at all times, including a smartphone, smart watch, tablet, and smart glasses. In the near future, mobile networks are expected to transmit more than 11 Exabytes of data per month [2]. Several technological candidates have proposed providing high data rate services to consumers. The Wireless Gigabit (Wi Gig) alliance recently proposed using the unlicensed 60 GHz frequency band to enable a 7 Gb/s short-range wireless connection. However, tracking techniques and advanced digital beam shaping are required for deployment in mobile wireless networks due to the substantial path loss of radio waves in this frequency range (60 GHz) [3].

Due to the high cost and scarcity of the Radio Frequency (RF) spectrum, innovative and complementary wireless transmission techniques are needed to alleviate the RF spectrum. There is a prospective band of the electromagnetic spectrum (i.e., the optical band) in the near future that can supply consumers with tens of gigabits per second [4], especially for indoor users. More than three decades ago, the first Optical Wireless (OW) systems were proposed as an alternative to RF systems for maintaining high data rates [5]. Since then, a large and growing amount of study has emerged in this sector, and in the last ten years, OW contact has grown in popularity as a high-potential.

Local area network speed approach in the last mile of network connectivity[6-13]. An OW devices are ideal candidates for high data rates. A VLC device based on white Light Emitting Diodes (LEDs) is one of the most promising OW systems for realizing universal wireless networks since LEDs can be used for both illumination and data communications. The dual functionality of a VLC system, namely illumination, and communication, makes it a very appealing technology for a variety of indoor and outdoor applications, including LED-based vehicle -to- vehicle communication, lighting infrastructures in buildings for high-speed data communication, and high-data-rate communication in airplane cabins [14].

The development of VLC systems has been aided by the recent invention of solid state lighting (SSL), which will provide high brightness LEDs of about 100 lx and 200 lx in the near future [15], with a longer lifespan (about six years) than traditional light sources, such as incandescent light bulbs (lifetime is about four months). SSL also has a

quick response time uses little power, and poses no health hazards. Figure 1.1 depicts the realistic luminous efficacy of many accessible light sources.

Red-Green-Blue (RGB) LEDs are used to get white LED as shown in Fig. 1.2. White color can be produced by combining three colors (RGB) correctly, as in color television [16].

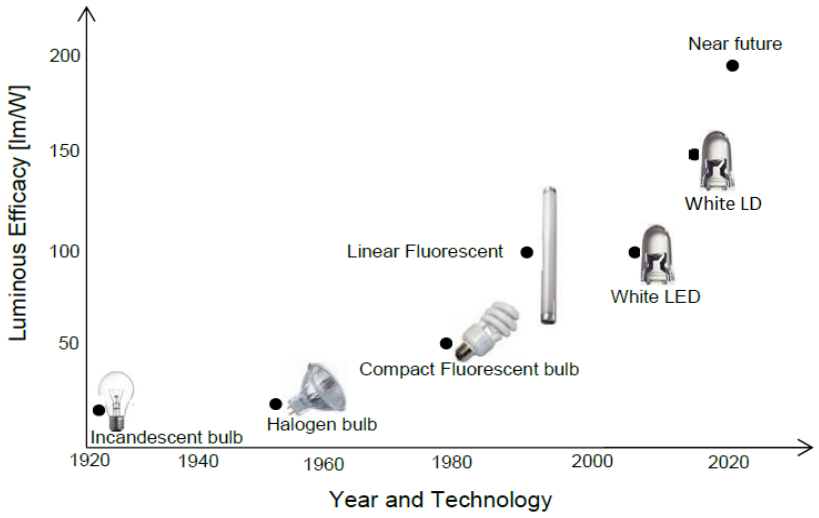

Figure 1.1: Compared of different light sources in term of luminous effectiveness [16].

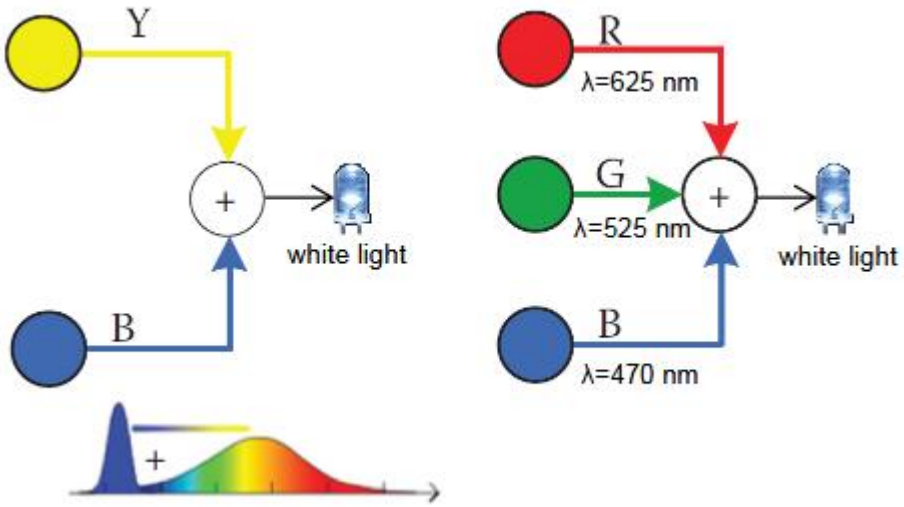

Figure 1.2: RGB method [16]

1.2 Motivation

To achieve the best light-based communication between users and internet service providers, it must determine the best way for the light to reach users. Obstacles between sender and receiver are one of the issues that will reduce the quality and speed of communication. To improve channel capacity and achieve higher SNR and BER, it is necessary to decide the receiver's location and use MIMO techniques.

1.3 Problem Statement

The radio spectrum is so crowded and finding a radio communication capacity to handle wireless data transmissions for media applications is becoming very difficult. Also, radio waves are costly, have only a limited range of bandwidth, require more energy, and

cause Electromagnetic Interference (EMI). Thus, VLC is an efficient and safe solution to overcome the above problems of Radio waves. VLC has a bandwidth of 400 THz (375-780 nm) which is significantly greater than the RF spectrum. Furthermore, the entire massive bandwidth can be reused without hindrance next door.

1.4 Thesis Objectives:

- Propose and test new approaches for improving the performance of optical communication systems when multipath dispersion and mobility are present.
- Design and model indoor mobile optical communication systems that function at greater data speeds (i.e., 5, 10, 20 Gb/s and beyond).
- Test the advantages of using angle diversity in a VLC system.
- Improve the SNR and reduce delay spread.

1.5 Contributions

1. Instead of light emitting diodes, RGB laser diodes (LD) were employed, researched, and evaluated for communication and illumination in VLC systems.
2. Proposed an 8×8 optical OFDM system based on MIMO to operate in the existence selective channel.
3. Eliminate interference from several users.

1.6 Scope of Work

Block diagram given in Fig. 1.3 summarized the scope of the thesis.

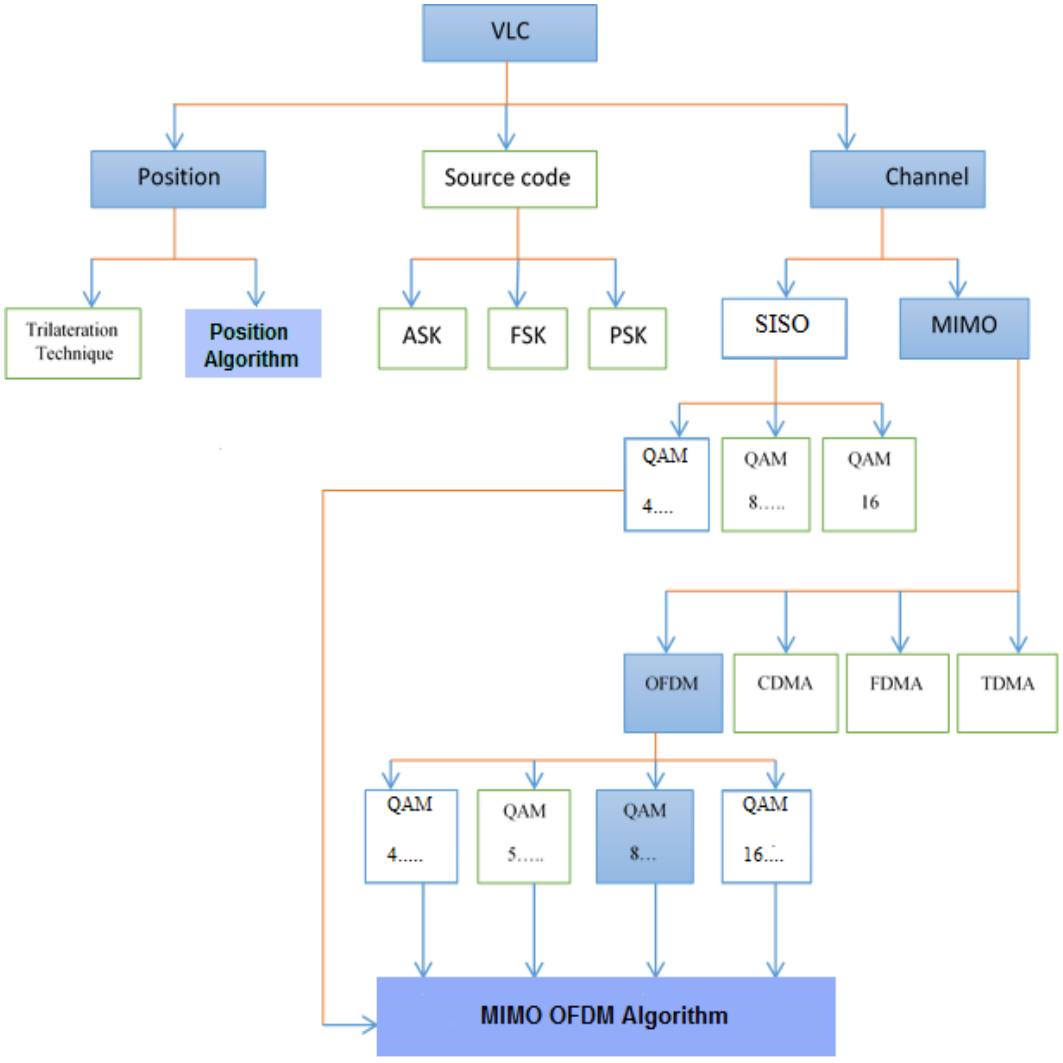

Figure 1.3: Block diagram of the scope of the work

1.7 Thesis Outline

Chapter1: VLC system: a general overview and characteristics in addition to a problem statement and an objective thesis

Chapter2: The history of the VLC system is discussed in terms of the approaches utilized by the researcher and the results produced in past years.

Chapter3: describes our process, which is broken down into two sections. The first section is used for location, while the second is used for channel coding.

Chapter4: describes the results that were achieved using the method described in Chapter 3.

Chapter5: gives discusses, conclusions and further works.

CHAPTER TWO

Literatures Survey

2.1 Introduction of VLC Systems

We all know that the spectrum is a valuable commodity among telecom experts. With the fast rise of wireless communication, the issue of spectrum utilization has become more efficient. To tackle this difficulty, a variety of solutions have been presented. One of these options is to transfer data using visible light frequencies. These frequencies are currently available and unoccupied. A novel wireless short-range optical communication technology that uses LEDs to transport data according to optical light characteristics to provide connectivity within a local area network.

VLC's features are described in depth below, along with why it is a viable alternative to wireless communication technologies. The most notable features of VLC's were compiled as follows:

- Low cost
- Low energy consumption
- Unorganized huge bandwidth

2.2 VLC Applications

Applications for both indoor and outdoor areas are covered by VLC devices. Data communications, indoor location prediction, indoor navigation for visually disabled people, and precise position measurements are examples of indoor applications. Outdoor applications include transportation, position data, and data conveyed via traffic signal infrastructure that adheres to the JEITA CP-1222 standard, Hazards to the climate, protection and defense, precise robot control, and aviation [17]. VLC systems, like Infrared Optical Wireless (IROW) systems, can be used to move data between offices. In an indoor area, user position can be estimated corridor are assumed to be illuminated by LEDs with a unique ID for each LED, utilizing white LEDs.

LEDs that are white, in combination with geometric sensors built into smart phones, may be able to assist visually for disabled people in moving around inside buildings. Figure 2.1 depicts a navigational prototype device as a visual aid disabled citizens [18]. RF signals, in particular, can be unwelcome in hospital settings. As a result, VLC devices may be possible solutions in operating rooms and magnetic resonance imaging (MRI) scanners.

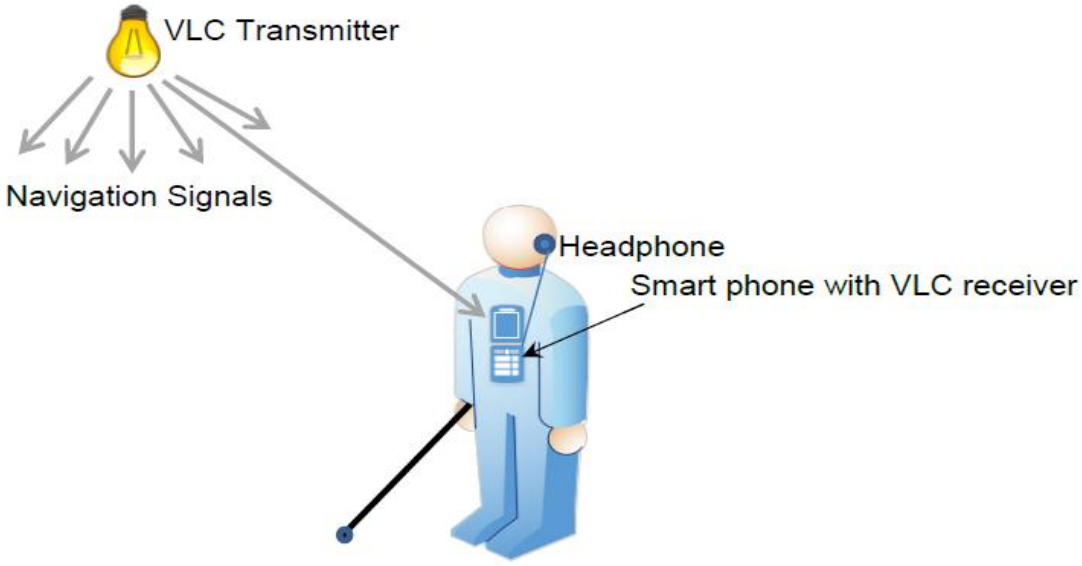

Figure 2.1: Indoor VLC navigation system for visually impaired people[16].

A number of VLC indoor positioning system techniques have been examined [19, 20]. Because of their many advantages, VLC systems have a lot of potential indoor positioning solutions. First, relative to radio wave systems, VLC has greater positioning accuracy (a few millimeters) because it suffers from fewer multipath effects and interference. Second, Where radio positioning systems are prohibited, VLC positioning systems can be employed, hospitals, for example [21]. In the automotive sector, Digital data can be transmitted using white LEDs (car-to-car communication), head and tail LED lights can be used to communicate between vehicles, and cars and traffic light infrastructure can also be communicated with [22].

2.3 Indoor VLC System Structure

Figure 2.2 depicts an indoor VLC system. (1) a white LED or visible LD transmitter, (2) a VLC channel (VLC links architecture), and (3) a photodetector (PD) receiver make up the VLC system. In the transmitter and receiver structure, digital and analog components are used. The digital components in the transmitter are the data stream, baseband modulator, and digital to analog converter (DAC). The analog to digital converter (ADC), demodulator, and data sink are all receiver's digital components. The transmitter's similar components are the trans-conductance amplifier (TCA), bias tee, and LED/LD.

The PD, trans-impedance amplifier (TIA), and band pass filter (BPF) are all part of the receiver. A bias tee in the transmitter adds the AC signal to the DC current (an injector of DC power into a high-frequency transmission line). Since LEDs use unipolar driving currents in a linear field, The total driving current must be larger than zero (AC+DC).

To emit the modulated output power, The LEDs receive the complete current. The PD converts the power it generates into a current (I-PD), which is made up consisting of two parts: AC and DC. TIA and BPF are used to amplify and filter the AC portion, respectively. After conversion with ADC, the digital signal is finally demodulated [23]. The VLC transmitter's primary role is to transform an electrical signal into an optical signal, which is then launched into the link for free space.

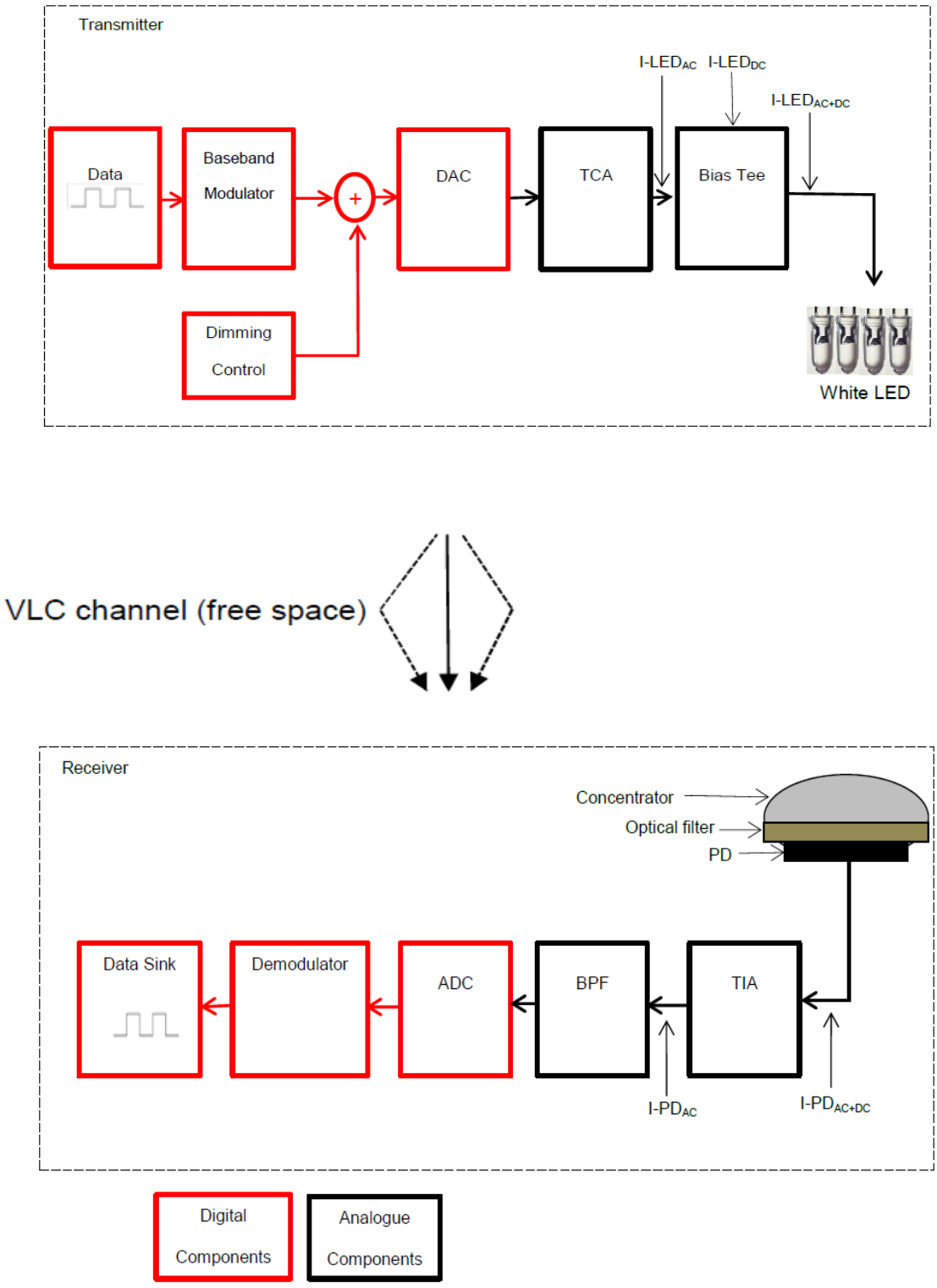

Figure 2.2: Block diagram of VLC system[16].

The obtained optical signal is converted into an electrical signal by a VLC receiver. It consists of a pre-amplifier circuit with a photodetector hidden behind the scenes of a front end. An optical filter with a concentrator makes up the front end. At the receiver, the concentrator raises the volume of power of the received signal [24-27].

VLC transmission is presently carried out using LEDs [28]. White LEDs are inexpensive and, even at reasonably high forces, are considered eye-safe. This is due to their large surface area, which allows them to emit light over a broad spectral range [28]. Light from commercial white LEDs is emitted in semi angles ranging from 12^{o} to 70^{o} [29]. In comparison to incandescent light bulbs, they are much more economical and efficient. As a result, LEDs are the preferred light source for indoor applications.

LEDs have some advantages, but they also have several disadvantages, such as [30]:

• Modulation bandwidth is limited (typically tens of MHz).

• Inefficient electro-optic control transfer (typically 10 to 40 percent).

• Non-linearity

Although LD is more costly than LED and require a more complicated drive circuit, it can be used for VLC systems instead of LED because of the various benefits, which includes:

• Wide-bandwidth modulation (typically hundreds of MHz to more than 10 GHz).

• High performance of electro-optic power transfer (30 to 70 percent of the time).

• Features of transfer of linear electrical to optical signals.

The degree to which the transmitter and receiver are pointing in the same direction, as well as a direct line between the transmitter and the receiver, are used to identify VLC connections. These categorizations are dependent on the transmitter's pattern of radiation and the receiver's field of view (FOV).

The two major types of indoor VLC links are a line of sight (LOS) and non-line of sight (NLOS) transmission configurations [31-33]. A direct path between the transmitter and receiver is provided by LOS connections, reducing the dispersion of several paths and increasing the VLC communication system's power performance. Figure 2.3 shows the different link classification systems.

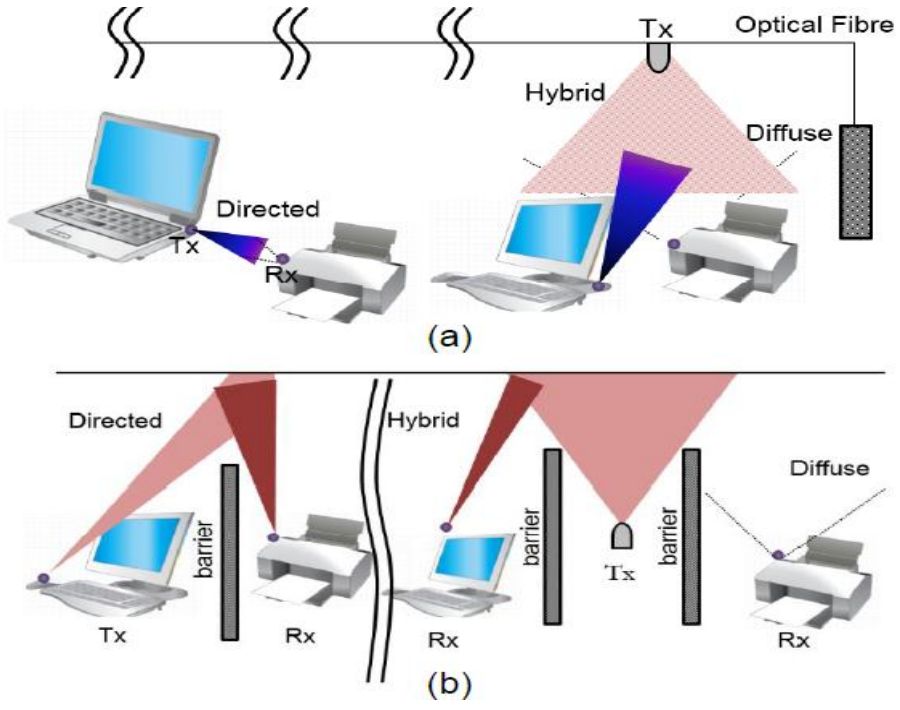

Figure 2.3: The two most common VLC connection configurations are (a) LOS transmission and (b) NLOS transmission[16].

The optical filter reduces the quantity of ambient light recorded by suppressing light captured outside the signal optical spectral range [34-38]. The photodetector is a key component in a VLC receiver because it converts the signal received via optical, which is interpreted directly into an electric current as "1" and "0" bits

2.4 Comparison between Visible Light Communication and Radio Frequency

VLC and RF systems both offer benefits and drawbacks that must be properly considered. Different applications prefer the use of one medium over the other, hence VLC and RF systems are complementing transmission approaches. In applications needing long-distance transmission or transmission through walls, as well as maximum user mobility, RF is ideal. VLC, however, When aggregate system capacity must be maximized at the lowest possible cost, or receiver signal processing complexity must be kept to a minimum, is chosen in short to medium link applications.

The majority of today's wireless communication systems are based on RF. However, the expanding There is demand for more frequency, cheaper components of cost, larger data rates, and improved QoS has compelled researchers to investigate another possibilities, like VLC. Compared to RF, VLC has a number of major advantages. For example, similar to fiber optic, a quick deployment, inexpensive startup operations costs, and increase bandwidth are all advantages. The VLC spectral region provides almost infinite bandwidth (380-780 nm), which is an unregulated global spectrum, resulting in lower system costs. Because of the way light works, the VLC system is immune to

interference from neighboring channels and allows for frequency reuse in various portions of a similar structure, resulting in plentiful capacity. The VLC system as well provides a stronger physical layer of security because light does not pass through opaque obstacles, making eavesdropping impossible, as is the case for radio systems. Benefits include the availability of low-cost basic front end devices, Hundreds of terahertz of license-free bandwidth, and energy efficiency, safety for people and electronic devices equipment, and ease of integration into existing lighting infrastructure. VLC systems are free of fading since the photodiode (detector) is very vast in dimensions, generally, tens of thousands of wavelengths [31,39], and the lack of fading can substantially the design of VLC systems much easier.

There are certain drawbacks to using a VLC system. Because a light is unable pass from one room to another through walls, a VLC point of access connected by a wired backbone will need to be built. Furthermore, the SNR is degraded by the spread of the received pulse caused by multipath dispersion. Reflective surfaces such as ceilings, doors, windows, and walls are responsible for multipath dispersion. The receiver receives the transmitted data from numerous various channels because these reflective components operate as miniature emitters that disperse a Lambertian pattern is used to represent the signal, which spreads the transmission pulses [12]. Furthermore, shot noise created by bright light sources in the environment (sunlight and other light sources) is included in the received signal at the receiver, resulting in signal distortion by background noise [40, 41]. Furthermore, when compared to the VLC spectrum, The transmitters' (LEDs) present modulation bandwidth is extremely limited, implying that bandwidth for transmission is constrained bandwidth of LEDs. Furthermore, since communicating with white LEDs is

inherently a one-way connection (downlink), which is excellent for purposes such as background music broadcast, It can be challenging to provide an uplink to a portable transmitter construction.

To attain satisfactory performance, a photodetector with a broad photosensitive surface is required for a VLC system. However, the capacitance of a photodetector is directly proportional to its area, i.e., a large photosensitive area results in a higher capacitance, reducing the receiver's possible bandwidth [42]. Table 2.1 illustrates a comparison between Wi-Fi and Li-Fi systems in indoor wireless Communications while the comparison of LD and LED systems is summarized in Table 2.2.

Table 2.1: Comparison between Wi-Fi and Li-Fi systems in indoor wireless Communications

Wi-Fi	**Li-Fi**
Wi-Fi is based on waves.	visible light is required for Li-Fi to function.
Wi-Fi uses a wireless router to transmit data.	Li-Fi transmits data using an LED or LD light.
The issue of Wi-Fi was accompanied by the issue of a nearby access point.	Interference is not an issue with Li-fi waves transmission devices. IrDA devices are compatible with Li-Fi.
Lan 802.11 is compatible with Wi-Fi (a ,b ,n ,ac ,ad)	IrDA devices are compatible with Li-Fi.

Because Wi-Fi signals cannot be blocked by walls, data must be protected using more secure means.	Because Li-Fi cannot pass through barriers, data is safe and secure..
Wi-Fi gadgets are rather expensive.	The VLC system employs low-cost transmitter and receiver equipment.
Hygienic: The amplitude of radiofrequency transmission cannot be very large, because once it reaches a certain level, it becomes unstable and very dangerous to human health.	Human health is unaffected by Li-Fi signals.

Table 2.2: Comparison between laser diode (LD) and Light Emitting Diodes (LEDs)

	LD	**LED**
Electrical to optical Conversion	More efficient with no droop	Less than LD with Droop
Bandwidth modulation	High	Lower
Modulation speed	High	Lower
Security	High	Less than LD
Coverage area	Less than LED	More

Emitting	Stimulated	Spontonuse
Life time	Longer life time	Lower than LD
Link distance	High	Lower
Link SNR	High	Lower
Cost	High	Lower
Power consumption	Low	Higher than LD

2.5 Literatures Survey

VLC system standardization began in Japan in 2003. In 2007, the Japanese electronics and information technology industries organization (JEITA) proposed two VLC standards, CP-1221 and CP-1222, respectively [43, 44]. The OMEGA project (home gigabit access network) was established in January 2008 as a result of major European initiatives to deliver high-bandwidth services for home area networks (the OMEGA project was funded by the European Commission) [45]. In the same year, the National Science Foundation (NSF) established the smart lighting engineering research center (ERC) in the United States [46]. Integrated standards have recently piqued the interest of many organizations, including IEEE. In September 2011, IEEE defined physical and media access control (MAC) levels for VLC systems. (802.15.7). The standard allows for

video and audio data rates of up to 96 Mb/s, as well as noise and interference from light sources [47]. In 2011, the light fidelity (Li-Fi) consortium, which is similar to Wi-Fi, was founded in Norway.

There were several researches that related with the work proposed in this thesis. some of them were summarized as following:

In 2014 Hameed & Shukla [48] ultrahigh capacity wireless optical communication systems have been discussed, with Li-Fi coverage services covering a larger area than Wi-Fi approaches. The Li-Fi wireless coverage service area has an ultra-high bandwidth of 5GHz, whereas the Wi-Fi wireless coverage service area has a bandwidth of 700MHz. With optical wireless communication or visible light communication, there is a multi-optical channel that provides ultrafast processing data rates (Li-Fi).

In 2017 Huichao Lv et al. [49] a differential detection-based positioning approach is proposed to improve the accuracy even more. It may eliminate positioning instabilities caused by light intensity fluctuations, and it can also position the area outside the light-emitting diode (LED) cell. The proposed method can enhance positioning accuracy from 10.0 to 4.0 cm and reduce standard deviation from 9.0 to 2.5 cm, according to experimental data. Outside the cell, however, location accuracy can be as low as 10.0 cm.

In 2018 Thomas Little et al. [50] to examine and optimize dense LiFi systems, a new multi-cell illumination test was developed. They created a system model with the goal of predicting signal strength under various navigation directions and in the future. Finally,

they show how the analytical model and measured data may be utilized to investigate VLP and VLC RSS-based delivery in multicellular systems using the analytical model and measured data.

In 2018 Sheng Zhang et al. [51] used ratio RSS with a neural network location estimator was used to demonstrate GPS for indoor 3D visual light. In a test area of 0.8 x 0.8 x 0.6 m3, sub-decimeter accuracy is attained.

In 2018 Imran Khan et al. [52] current WLAN and the prospective WLAN are compared in terms of general and technical standards, as well as differences in advantages and disadvantages. It has been determined which method is the most effective in meeting future communication needs.

In 2019 Abdullah Ali Qasimet al. [53] a summary of the significant advancements in the field of semiconductors was presented, with a focus on the light-emitting diode (LED) and laser diode (LD), which are used for illumination and communications at the same time. The features of optical signal modulation schemes were also examined and compared. In the VLC system, they also worked on creating and implementing FBMC (Multi-Vector Filter Bank) technology. VLC is a contender for the future generation of communications, which will be developed for both domestic and international use.

In 2019 Yinzhou Tan et al. [54] IMIDD was compared to LiFi and coherent LiFi systems using symmetric detection and direct current biased orthogonal frequency division multiplexing (DCOOFDM). The two systems' BER performance and energy

efficiency measures are compared. The channel (DC) direct current gain characteristics of the two systems are also investigated. The simulation findings reveal that the coherence system outperforms the IMIDD system in terms of bit error rate (BER), however, the coherent system's transmitter and receiver must be identical. In addition, the coherent system is more energy efficient than the IMIDD system in the same coverage area.

In 2019 Mohammed S.M. Gismalla et al. [55] the regularity of the internal VLC system is improved in terms of high received power, signal-to-noise ratio (SNR), and bit rate, while the spread of the RMS delay has been reduced. It has a new rooftop model that uses the ATOS 13 optical setup. In addition, the proposed model was tested at a different angle and at half the force. The average received power and SNR were improved to 2.85 dBm and 75.5 dB, respectively, while the received power levels and SNR in the center of the room were 4.92 dBm and 79.5 dB. 211 MB/sec, with a minimum mean RMS propagation delay of 0.4749 ns. The proposed concept improves connection quality while also meeting lighting requirements.

In 2019 Cătălin Beguni et al. [56] a brief review of OWC technologies is provided and a focus on their use in automated applications. On the basis of a standard vehicle lighting system, they recently developed vehicle visible light communication systems and visible light range systems in order to set a path toward designing hybrid visible light communication systems and distance control systems for automotive applications.

In 2019 Radek Martinek et al. [57] the initial attempt was presented in LabVIEW as a visual optical communication system based on a Software Defined Radio (SDR). The two

most frequent varieties of LED headlights, roof lights, and LED headlights/taillights, The focus of this paper will be on that. The primary goal of this research is to identify the fundamental parameters for a successful VLC implementation, such as transmission speed and communication failures (bit error ratio, error vector size, power per bit to noise spectral density ratio.) Also, the greatest distance can be covered.

In 2020 Sathisha R N et al. [58] demonstration of high-quality real-time multimedia data streams using a laser-based internal optical communication (VLC) link with a remote stimulated blue laser phosphorous as a transmitter, a silicon accumulator photodetector as a receiver, and USRP platforms for data/extract manipulation. The VLC link is identified separately and has a bandwidth of > 800 MHz. With an Ethernet link data rate of 200Mbps and an RF bus frequency of 245MHz at the front end of the radio, an HD video stream of 1280 x 720 quality was successfully presented via this VLC link.

In 2020 Saif N. Ismail & Muataz H. Salih. [59] VLC will be convenient and easy to control sync like light and data, according to a study presented, explained, and discussed. VLC is a potential and practical complementary innovation to remote radio frameworks for future short-term applications.

Table 2.3 summarizes the literature review that is closest to the work of this thesis.

Table-2.3 Summary of Literature Review

No	Year	Researcher	Method
1	2011	TIAN Chong-wen et al.	Using a white LED matrix, the OFDM/VLC system is designed and the transceiver is designed by the MATLAB/Simulink instrument, and the detector response is derived according to the Lambert model. The effects of factors including digital modulation, RS coding, pilot shape and connection distance on system performance are discussed. The results show that the bit error rate can be reduced to less than 10-5, and the communication distance can reach 0.9m.
2	2017	Ton Koonen et al.	An educational overview is provided on two major trends in OWC: wide recovery visible light communication based on LED lighting technologies and sharing the capacitance between multiple devices, and communication with 2D narrow infrared beams that provide high capacity non-shared devices individually. In addition, technologies supporting wide field of view receivers, device localization, two-

			way hybrid optical / radio networks, and two-way optical wireless networks are discussed.
3	2018	Michael Rahaim et al.	A new multi-cell lighting test created to study and optimize dense LiFi systems. We are developing a model of the system with the purpose of predicting signal strength under different navigation and future directions. The data collected on the test shows a good fit with the model. Finally, we demonstrate how the analytical model and measured data can be used to study VLP and VLC RSS-based delivery in multicellular systems.
4	2018	MOSTAFA ZAMAN CHOWDHURY et al.	A technology overview and review of optical wireless technologies, such as visible light communications, light, optical camera communications, free-space optical communications, and the detection and range of light are presented. Art standards in aspects such as classification, spectrum use, architecture and applications.

5	2019	Cătălin Beguni et al.	A brief overview of OWC technologies is presented and focused on their use in automated applications. Thus, vehicle visible light communication systems and visible light range systems recently developed by our research groups in order to determine the path towards the design of mixed visible light communication and rangefinder system for automotive applications are presented on the basis of a standard vehicle lighting system.
6	2019	D. Plets et al.	Accuracy of a 3D visible light positioning (VLP) algorithm for different LED configurations employing the same four lamps but installed in different places on the ceiling. Average errors of 12.7 cm and maximum errors of 21.1 cm are found experimentally for LEDs around 3 m above the receiver, demonstrating the viability of 3D VLP for unmanned navigation.
7	2019	Abdullah Ali Qasim	A summary of the significant advancements in the field of semiconductors was presented,

		et al.	with a focus on the light-emitting diode (LED) and laser diode (LD), which are used for illumination and communications at the same time. The features of optical signal modulation schemes were also examined and compared. In the VLC system, they also worked on creating and implementing FBMC (Multi-Vector Filter Bank) technology. VLC is a contender for the future generation of communications, which will be developed for both domestic and international use.
8	2020	Alain R. Ndjiongue et al.	The feasibility of using VLC as a network technology was considered and the challenges related to implementing a VLC-based network, as well as integrating VLC into existing traditional networks, were discussed and included in the standards.

CHAPTER THREE

Methodology of the Proposed Visible Optical Communications System

3.1 Method Outline

This work is divided into two parts. The first part includes designing an optical communication system consisting of 5 laser sources for transmission with building a new algorithm to find the best-received power relative to the location of the receiver and thus finding the best value for the SNR. In the second part, a new algorithm is designed to the MIMO system in channel coding using OFDM for 8 laser sources. This is done using Matlab software.

3.2 Positioning and Reflected Algorithm

3.2.1 Laser VLC System and Room Setup

The suggested VLC systems designed here is consist of a vacant room of 6 × 6 × 3 m (width, length, and height) and white LD which emits a beam of red, green, and blue wavelengths (Figure 3.1). Five RGB-LD lighting units are used to illuminate the area, which is set in regular forms so that the four sources (1, 2, 3, 4) were dispersed 1.5 m apart along the room's ceiling borders. The fifth and final source (5) is located in the center of

the ceiling. It has been used to ensure compliance with ISO (International Organization for Standardization) and European standards [60]. Because each LD laser diode is a 25 (5 x 5) RGB-LD, there are 125 LDs in the room. The LDs are suspended three meters above the ground. A reflecting object (like mirror) with area of 0.025 m^2 is placed on one side of the room, and its effect on the signal strength and consequently the SNR value will be investigated.

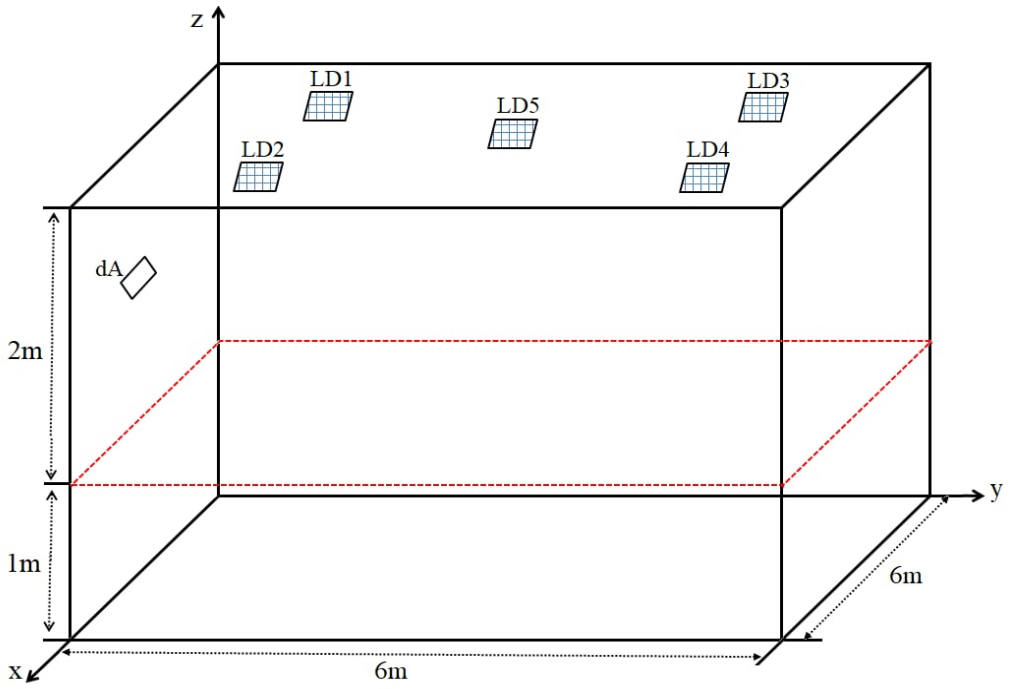

Figure 3.1 Room equipped with 5 laser diode sources with reflector

The parameters in the proposed system took into account the power line-of-sight (PLOS) and power-first-order reflections (PFST) of a 1m high VLC transmitter for a receiver and a reflector until the received SNR value was optimized by increasing the power, as illustrated in the next items**.**

3.2.2 Calculations of received optical power

As a result of multipath propagation, there may be more than one path between the transmitter and the receiver. Multiple pathways in the optical transmission cause temporal dispersion in the signal. The received optical power can be calculated using a ray tracing technique. All possible pathways for reflected optical beams from different reflectors to other reflectors or the receiver are traced. As a result, surfaces reflecting are separated into a number of equal sized (square_shaped) reflection elements in order to implement ray tracing. The Lambertian pattern (n = 1) is formed by the optical rays reflected from these elements. The accuracy of the impulse response is improved by the small size of these elements. When the size of the surface element is reduced, however, the computing time increases considerably. At the receiver, the total received optical power (Pr) includes the PLOS and PFST, is calculated as follows:

$$P_r = \sum_{i=1}^{S} P_{LOS} + \sum_{i=1}^{M} P_{FST} \quad (3.1)$$

In a first-order reflection, *S* signifies the number of transmitter units and *M* specifies the number of reflecting elements.

The LOS ray tracing setup, as well as first and order reflections, are shown in Figure 3.2. The VLC channel's impulse response can be calculated by tracing all possible light rays between the transmitter and the receiver.

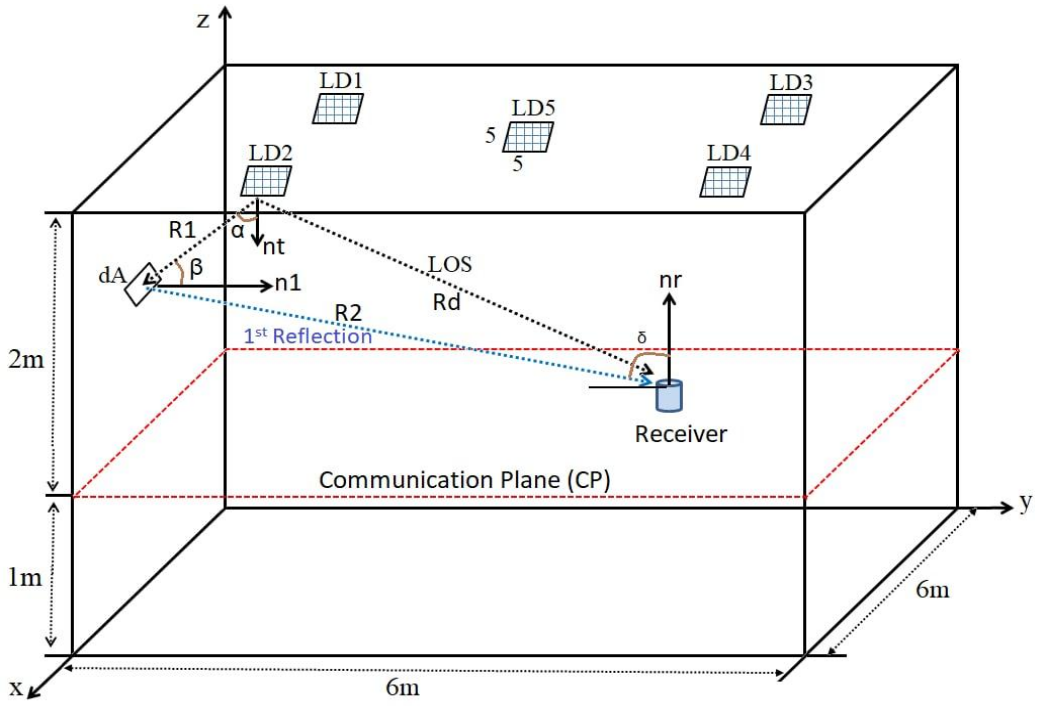

Figure 3.2 VLC system, ray tracing setup for LOS, first order reflections

3.2.3 Line-of-Sight (LOS) Analysis

When the transmitter and receiver are connected by a direct path, an LOS component is available. For example, in a VLC system, the PLOS component can be stated as shown in Figure 3.3 which gives the transmitter on the ceiling with an elevation angle of -90^o (facing downwards) and the receiver on the communication plane with an elevation angle of 90^o (looking upwards). PLOS can be written as[16]:

$$P_{LOS} = \begin{cases} \frac{n+1}{2\pi R_d^2} \times P_S \times cos^n(\alpha) \times cos(\delta) \times A & 0 \leq \delta \leq \psi_c \\ 0 & \delta > \psi_c \end{cases} \quad (3.2)$$

where *Ps* denotes the total average transmitted optical power radiated by the light source (LD), A denotes the detector area, δ is the angle between the photodetector's normal and the incident ray, α the angle formed by the transmitter's normal and the ray of irradiance, and R_d denotes the distance between the transmitter and the receiver. The direct LOS received power approaches 0 when the received angle (δ) is greater than the semi-angle of acceptance (ψc). Because the signal must fall within the receiver's field of view (FOV) in order to be received, adjusting the FOV of the receiver can be utilized to reduce noise (light in the background) and undesirable reflections.

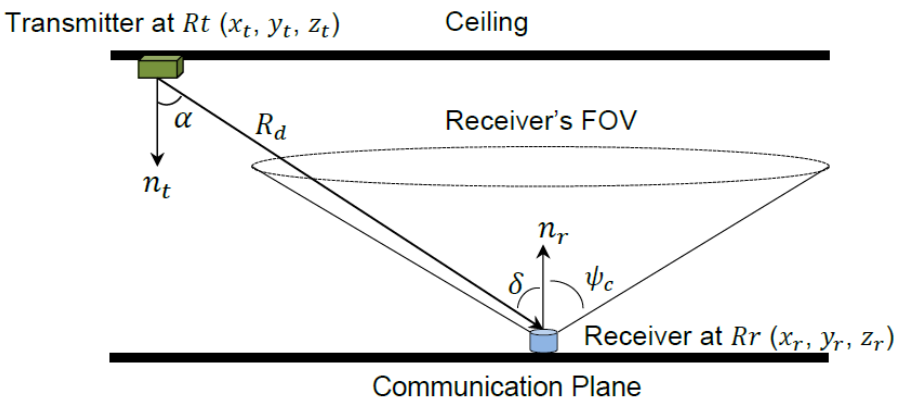

Figure 3.3 Ray tracing for the LOS.

where $\hat{nt}$ is the transmitter's normal at location *Rt* and $\hat{nr}$ is the receiver's normal at location *Rr*. It's worth noting that if the transmitter and receiver are in parallel planes, as shown in Figure 3.2. The transmission and receiving angles are different if the $\hat{nt}$ is vertical to the $\hat{nr}$, or normalized. When calculating these angles, both scenarios are taken into account. *Rd* is the direct distance between transmitter and receiver, which can be computed as follows[16]:

$$Rd = \| Rr - R \| = \sqrt{((xr - xt)^2 + (yr - yt)^2 + (zr - zt)^2)} \quad (3.3)$$

where the transmitter and receiver coordinates are x_t, y_t, z_t and xr, yr, zr, respectively.

3.2.4 First Order Reflection Analysis

Figure 3.4 depicts a ray emitted by the transmitter and reflector element to the receiver. With ne = 1 plaster walls can be thought of as Lambertian reflectors [5]. The Lambertian model can be used to compute the received optical power of first order reflections P_{FST} as follows[16]:

$$P_{FST=} \begin{cases} \frac{(n+1)(ne+1)}{4\pi^2 R_1^2 R_2^2} \times P_S \times \rho_1 \times dA_1 \times cos^n(\alpha) \times cos(\beta) \times cos^m(\gamma) \times cos(\delta) \times A & 0 \le \delta \le \varphi_C \\ 0 & \delta > \varphi_C \end{cases} \quad (3.4)$$

where R_1 denotes the distance between the transmitting and receiving elements, R_2 denotes the distance between the receiver and the reflecting element, and α is the angle formed by the normal of the transmitter and the irradiance ray. β the angle formed by the transmitter's irradiance ray and the normal of the reflecting element, γ is the angle formed by the normal of the reflecting element and the reflected ray towards the receiver, δ and is the angle formed by the receiver's normal and the incident ray. The size of the reflecting element is dA_1, and the reflective surface's reflection coefficient is ρ_1.

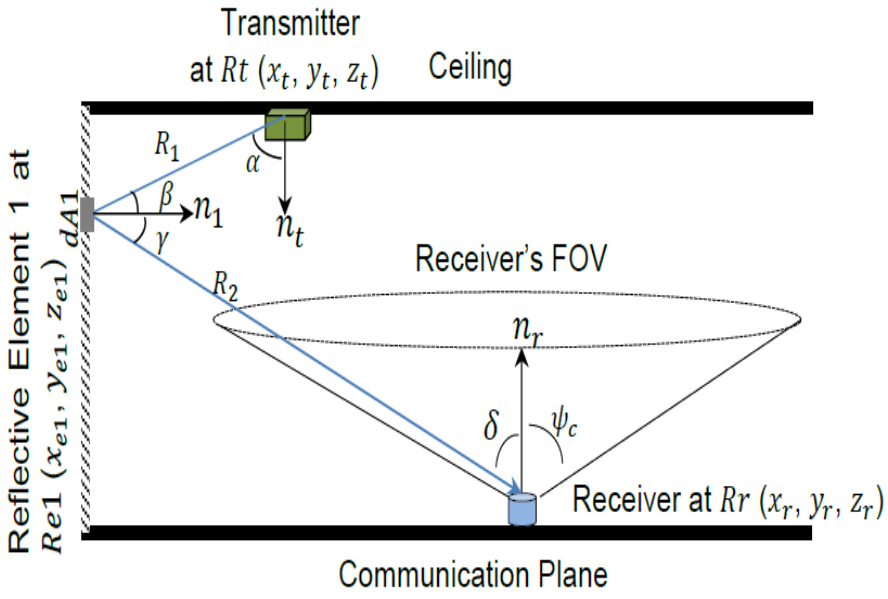

Figure 3.4 Ray tracing for the first order reflections

The reflecting elements are viewed as secondary tiny transmitters, with the retransmitted power defined by the received optical power and the reflection coefficient of the transmitter of ρ_1. Equation 3.4's four angles can be calculated as follows:

$$\cos(\alpha) = \hat{nt} \cdot (Re_1 - Rt) / R_1 \qquad \cos(\beta) = \hat{n_1} \cdot (Rt - Re_1) / R_1$$

$$\cos(\gamma) = \hat{n_1} \cdot (Rr - Re_1) / R_2 \qquad \cos(\delta) = \hat{nr} \cdot (Re_1 - Rr) / R_2 \tag{3.5}$$

where $\hat{n_1}$ denotes the reflecting element 1's normal at Re_1. As for Table 3.1, it shows all the parameters that were used in this work.

Table 3.1 Positioning VLC parameters

Parameters	**Value**
Room dimension (L×W×H)	6×6×3 (m^3)
A_{RX} the photodiode aperture Area	0.5 mm^2

LD array Chip	5×5
P_{LD}	0.0002 w
dA_1 Area of the reflective element	$0.025m^2$
n Mode number	1

3.3 LD Index Modulation in Optical MIMO-OFDM

The VLC is a new technology for wireless communication networks of the future.For the MIMO and OFDM-based VLC systems, present a new generalized LD indication modulation approach was presented.

In this work a (6 × 6 × 3) m room and equipped it with 8 transmitting laser sources distributed over interconnected spaces in the room ceiling and tested them on 8 locations of the receiver using MIMO-OFDM technology where there are more than one output and more than one user at the same time. The study offered a new technology of maximum posteriori probability (MAP) Estimator with the aim of finding the best connection between the light source of the signal and the user by location by estimating the channel (H) values of each user according to the coordinates X, Y, Z.

The proposed system avoids the normal spectrum efficiency losses that occur in OFDM communications owing to time and frequency domain modulation. This is accomplished by utilizing the spatial multiplexing associated with LD index modulation.

As a result, the real and imaginary components of OFDM signals are split in the complex time domain first, and the resulting dipole signals are subsequently sent across the VLC channel using LD indexes to encode the signal information. For both physical and analytical channel models, present a test of our proposed system's performance as a benchmark. Computer simulations of a large scale have shown that the proposed approach outperforms conventional VLC-MIMO-OFDM systems with the same number of transceivers [LDs and photodiodes (PDs)] in terms of bit-error ratio and signal-to-noise performance. By utilizing the MIMO configuration, DC bias and spectral efficiency may be multiplied and separated, respectively, when compared to the DC-biased optical (DCO)-OFDM (SISO) system. Matlab software was used to perform simulations and calculations.

3.3.1 The Presence of Frequency-Flat MIMO Channels with MIMO-OFDM

The suggested system's a schematic diagram shown in Figure 3.5. Data bits carrying vector u enter the MIMO-OFDM transceiver for frequency-flat MIMO channels. For each OFDM block, a MIMO-OFDM transmitter is used, where N denotes the number of OFDM subcarriers and M denotes the signal constellation's size, Quadrature amplitude modulation in 8-ary, for example (8-QAM). OFDM modulator in the proposed scheme processes the complicated frequency-domain OFDM structure x_F directly without requiring Hermitian symmetry. $x_T = [x_1 \bullet \bullet \bullet x_N]^T$ is the time-domain OFDM frame that results. Because of its bipolar (positive and negative valued) and complex-valued parts, cannot be sent across a VLC channel. To be able to solve this issue.

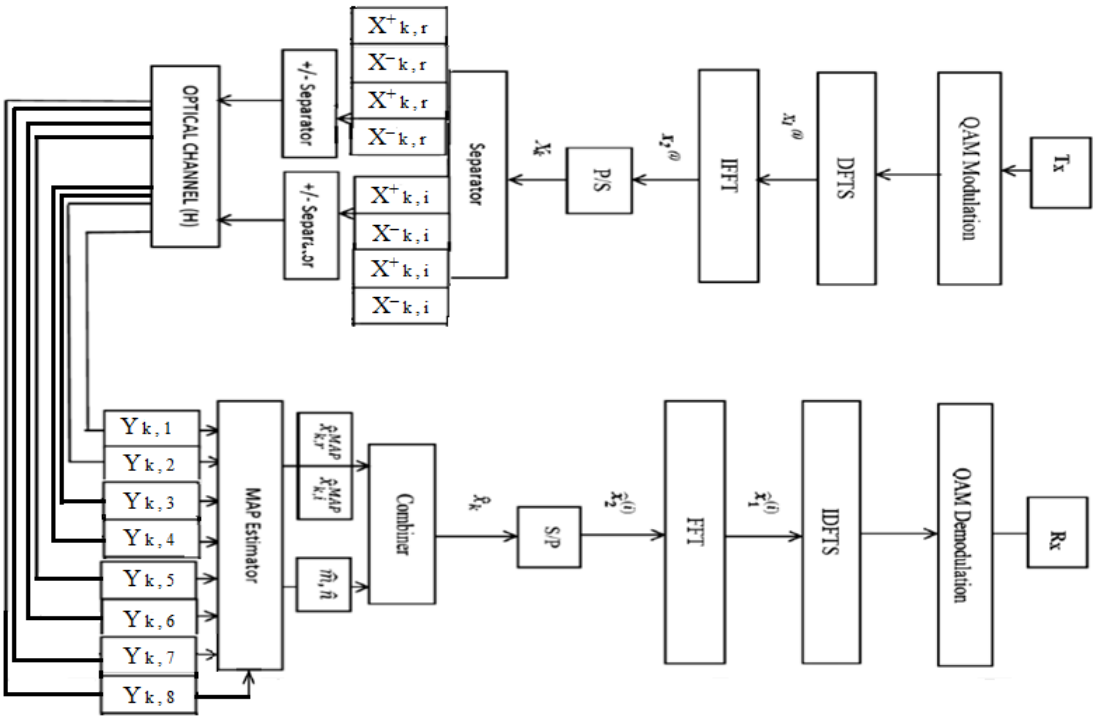

Figure 3.5 Block diagram of the MIMO-OFDM architecture for a VLC system with eight channels.

This work delt with a new MIMO transmission mechanism based on LD index modulation has been developed where no Hermitian symmetry and DC bias are employed in the modulation process to ensure that the baseband signals are in the real and imaginary domains to function through frequency flat optical channels. Signals will be delivered utilizing the active light-based modulation index across MIMO-Optical channels (LD). In addition, a unique MAP estimator is used at the receiver to calculate specific imaginary and real components of the OFDM signals. A MIMO transmission system is being developed to solve bipolar (positive and negative) elements values of the VLC channel. After parallel-to-serial (P/S) conversion, For each time-domain OFDM signal x_k, the real and imaginary components are separated as $x_k = x_{k,R} + j\ x_{k,I}$ using a like technique as in

ref. [61], where k = 0, 1,..., N - 1. The resulting positive real valued signals $x_{k,R}$ and $x_{k,I}$ are then processed by positive-negative (+/-) separators to create the real positive valued signals illustrated below [62]:

$$
\begin{aligned}
x_{K,R}^{+} &= \begin{cases} x_{K,R} & if\ x_{K,R} > 0 \\ 0 & if\ x_{K,R} < 0 \end{cases} \\
x_{K,I}^{+} &= \begin{cases} x_{K,I} & if\ x_{K,I} > 0 \\ 0 & if\ x_{K,I} < 0 \end{cases} \\
x_{K,R}^{-} &= \begin{cases} 0 & if\ x_{K,R} > 0 \\ -x_{K,R} & if\ x_{K,R} < 0 \end{cases} \\
x_{K,I}^{-} &= \begin{cases} 0 & if\ x_{K,I} > 0 \\ -x_{K,I} & if\ x_{K,I} < 0 \end{cases} \\
x_{K,R}^{+} &= \begin{cases} x_{K,R} & if\ x_{K,R} > 0 \\ 0 & if\ x_{K,R} < 0 \end{cases} \\
x_{K,I}^{+} &= \begin{cases} x_{K,I} & if\ x_{K,I} > 0 \\ 0 & if\ x_{K,I} < 0 \end{cases} \\
x_{K,R}^{-} &= \begin{cases} 0 & if\ x_{K,R} > 0 \\ -x_{K,R} & if\ x_{K,R} < 0 \end{cases} \\
x_{K,I}^{-} &= \begin{cases} 0 & if\ x_{K,I} > 0 \\ -x_{K,I} & if\ x_{K,I} < 0 \end{cases}
\end{aligned}
\quad \text{for eight sources} \qquad (3.6)
$$

MIMO VLC system with a $N_R \times N_T$ can transmit these signals concurrently, with n_T and n_R denoting the number of Rx (receiver) and Tx (transmitter) units, respectively. It's worth noting that the suggested strategy, n_T must be divisible by eight, which is why $N_T = 8$ is used in this study. LDs broadcast the absolute values of $x_{k,I}$ and $x_{k,R}$ signals in the MIMO -OFDM scheme, and the index of the transmitting LD determines the sign of the corresponding signals. MIMO-OFDM, on the other hand, totally avoids Hermitian symmetry at the IFFT input, as well as the resulting spectral efficiency loss. Because Hermitian symmetry is no larger necessary to produce real-valued OFDM symbols, signals from the $N_R \times N_T$ MIMO-VLC system can be broadcast simultaneously. For k =

0, 1,..., N - 1[63], OFDM time samples with a positive and real value $x_{K,R}^{+}$, $x_{K,R}^{-}$, $x_{K,I}^{+}$, and $x_{K,I}^{-}$ are communicated via the N_R=8 MIMO optical channel represented by (H).

$$\mathbf{y} = Hx + n \tag{3.7}$$

where $\mathbf{y} = \left[y_{K,1\ldots\ldots}y_{K,n\,R}\right]^T \in R^{NR}$ In the vector of received signals, the electrical signals collected from PDs at the Rx units are included. In Eq. (3.7), $n \in R^{NR}$ Models shot noise and thermal noise with a vector of additive white Gaussian noise (AWGN) samples with simulation values. The elements of **n** follows $N(0, \sigma_{w}^{2})$ In the electrical realm, they are combined with the received signals. The signal vector that is being conveyed $\mathbf{x} \in R^{8\times1}$ is formed for MIMO -OFDM as :

$$X = \left[x_{K,R}^{+} \quad x_{K,R}^{-} \quad x_{K,R}^{+} \quad x_{K,R}^{-} \quad x_{K,I}^{+} \quad x_{K,I}^{-} \quad x_{K,I}^{+} \quad x_{K,I}^{-}\right]^T \tag{3.8}$$

where the elements of x represent the signals emitted by the LDs. According to Eq. (3.6), only four out of eight x elements are non-zero for a given OFDM signal, i.e., The active LDs (those that emit light) are four, while the dormant LDs are four (turned off). As in the example, for $x_k = -2.1 + j3.8$, getting $\mathbf{x} = [0 \quad 2.1 \quad 0 \quad 2.1 \quad 3.8 \quad 0 \quad 3.8 \quad 0]^T$. The second and fourth LDs are active, conveying the real component of x_k absolute value, while the third and sixth LDs are also active, transmitting the positive imaginary part of x_k. From this approach, the suggested technique employs the index modulation principle to transmit complex OFDM signals using active LD indices. Using $n_R = 8$ in this study because it is easier to present, and generalization is simple. The LDs are presumed to be working within their dynamic range. Non-linear distortions are not present in the operation in Eq. (3.6). The optical MIMO channel of 8 x 8 is denoted by:

$$H=\begin{bmatrix} h_{1,1} & h_{1,2} & h_{1,3} & h_{1,4} & h_{1,5} & h_{1,6} & h_{1,7} & h_{1,8} \\ h_{2,1} & h_{2,2} & h_{2,3} & h_{2,4} & h_{2,5} & h_{2,6} & h_{2,7} & h_{2,8} \\ h_{3,1} & h_{3,2} & h_{3,3} & h_{3,4} & h_{3,5} & h_{3,6} & h_{3,7} & h_{3,8} \\ h_{4,1} & h_{4,2} & h_{4,3} & h_{4,4} & h_{4,5} & h_{4,6} & h_{4,7} & h_{4,8} \\ h_{5,1} & h_{5,2} & h_{5,3} & h_{5,4} & h_{5,5} & h_{5,6} & h_{5,7} & h_{5,8} \\ h_{6,1} & h_{6,2} & h_{6,3} & h_{6,4} & h_{6,5} & h_{6,6} & h_{6,7} & h_{6,8} \\ h_{7,1} & h_{7,2} & h_{7,3} & h_{7,4} & h_{7,5} & h_{7,6} & h_{7,7} & h_{7,8} \\ h_{8,1} & h_{8,2} & h_{8,3} & h_{8,4} & h_{8,5} & h_{8,6} & h_{8,7} & h_{8,8} \end{bmatrix} \quad (3.9)$$

where $h_{r,t}$ signifies the optical wireless link's channel gain between the Tx unity (LD) t and the Rx unity (PD) r, where (t, r) are {1, 2, 3, 4, 5 , 6 , 7 , and 8 }. For each ray, the observed power as well as the distance between the source and the detector are given [64].

$$h(t) = \sum_{i=1}^{Nr} pi\ \delta(t - \tau_i) \quad (3.10)$$

where *Pi* is the i^{th} ray's optical power, *i* is the i^{th} ray's propagation time, and *Nr* is the total number of rays that the detector has received.

$$I = \frac{1}{2(\sqrt{\pi})} \quad (3.11)$$

where I denotes the average optical intensity of the light emitted [65].

3.3.2 MIMO -OFDM with Conditional MAP Estimator

The model of transmission in Eq. (3.7) is similar to that of traditional single-carrier MIMO-SM systems, but it varies from them for two factors. The received signals in Eq. (3.7) real and the Gaussian distribution of the transmitted data vector x is clipped. Furthermore, because complex valued signals should be created first to acquire the estimation of OFDM block xF in the frequency domain, it isn't viable to send the received signal vector y directly to the OFDM demodulator. Employment of a zero-forcing (ZF)

equalizer, it yields an estimate of x simply. It is a simple solution to the problem of estimating described in Eq. (3.7).

$$\acute{x}^{ZF} = H^{-1}y. \tag{3.12}$$

Following this procedure, the receiver can choose the greater magnitude signals from $\acute{x}^{ZF}$ to determine the indices of the active LDs and related signals [66]. Despite the fact that it is simple, the ZF estimator can greatly increase noise power by multiplying n by H^{-1}. Also, it does not take into account x's probability distribution as prior information, therefore it may yield negative-valued estimates. To address the ZF estimator's shortcomings, For the MIMO-OFDM system, we propose a novel MAP estimator in this section, which takes into consideration the prior information we have for the signal vector x. The column vectors of the channel matrix H are used to define it as H = $\begin{bmatrix} h_1 & h_2 & h_3 & h_4 & h_5 & h_6 & h_7 & h_8 \end{bmatrix}$ Thus Eq. (3.7) observed signals can be rewritten as[65]:

$$y = h_m \tilde{x}_{K,R} + h_n \tilde{x}_{K,I} + n \tag{3.13}$$

where $\tilde{x}_{K,R} = |x_{K,R}|$, . $\tilde{x}_{K,I} = |x_{K,I}|$, $m \in \{1,2,3,4\}$ and $n \in \{5, 6,7, 8\}$. It is simple to demonstrate that. $\tilde{x}_{K,R}$ and $\tilde{x}_{K,I}$ have the following folded Gaussian (half-normal) distribution [65]

$$p.\, \tilde{x}_{K,R(I)}{}^{(v)} = \frac{2}{\sqrt{\pi}} e^{-v2}\, u(v). \tag{3.14}$$

As a result, the conditional MAP estimates of for a given pair (m, n) are. $\tilde{x}_{K,R}$and . $\tilde{x}_{K,I}$ can be gotten as [65]:

$$\left(\tilde{X}_{K,R}^{(m,n)}, \tilde{X}_{K,I}^{(m,n)}\right) = \arg\max \tilde{x}_{K,R}, \tilde{x}_{K,I}\; p\left(\tilde{x}_{K,R}, \tilde{x}_{K,I} \,|y\right) \tag{3.15}$$

where $p\left(\tilde{x}_{K,R}, \tilde{x}_{K,I} \mid y\right)$ is the p.d.f. of $\tilde{x}_{K,R}$and $\tilde{x}_{K,I}$, conditioned on **y**. Eq. (3.15) could be written as a result of simple adjustments.

$$\left(\tilde{X}_{K,R}^{(m,n)}, \tilde{X}_{K,I}^{(m,n)}\right) = \text{argmax } \tilde{x}_{K,R}, \tilde{x}_{K,I}\ M^{\text{MAP}}\left(m, n, \tilde{x}_{K,R}, \tilde{x}_{K,I}\right) \tag{3.16}$$

where $M^{\text{MAP}}\left(m, n, \tilde{x}_{K,R}, \tilde{x}_{K,I}\right)$ is the MAP estimation metric defined as:

$$M^{\text{MAP}}\left(m, n, \tilde{x}_{K,R}, \tilde{x}_{K,I}\right) = \left\|y - h_m \tilde{x}_{K,R} - h_n \tilde{x}_{K,I}\right\|^2 + 2\sigma_{\text{w}}^2\left(\tilde{X}_{K,R}^4 + \tilde{X}_{K,I}^4\right) \tag{3.17}$$

Using $\|a\| = a^T a$ and after a little math, Eq. (3.17) can be simplified as:

$$M^{\text{MAP}}\left(m, n, \tilde{x}_{K,R}, \tilde{x}_{K,I}\right) = A\,\tilde{X}_{K,R}^4 + B\tilde{X}_{K,I}^4 + C\tilde{x}_{K,R} + D\tilde{x}_{K,I} + E\tilde{x}_{K,R}\,\tilde{x}_{K,I} \tag{3.18}$$

where

$$A = h^T_m h_m + 2\sigma_{\text{w}}^2 \qquad B = h^T_n\, h_n + 2\sigma_{\text{w}}^2$$

$$C = -2y^T\, h_m \qquad D = -2y^T\, h_n$$

$$E = 2h^T_m h_n \tag{3.19}$$

Calculating $M^{\text{MAP}}\left(m, n, \tilde{x}_{K,R}, \tilde{x}_{K,I}\right)$ derivative with respect to $\tilde{x}_{K,R}$and $\tilde{x}_{K,I}$and Equating to zero produces the following MAP estimates for$\tilde{x}_{K,R}$and $\tilde{x}_{K,I}$, conditioned on *(m, n)*:

$$\tilde{X}_{K,R}^{(m,n)} = \left[\frac{2BC - ED}{E^2 - 8AB}\right]^+ \quad , \quad \tilde{X}_{K,I}^{(m,n)} = \left[\frac{2AD - EC}{E^2 - 8AB}\right]^+ \tag{3.20}$$

To identify the active LDs' indices (i.e., m , n estimations) as well as the associated estimates of $\tilde{x}_{K,R}$ and $\tilde{x}_{K,I}$, the conditional MAP estimator determines $\tilde{X}_{K,R}^{(m,n)}$and $\tilde{X}_{K,I}^{(m,n)}$ for each of the possible (m, n) pairs, and then calculates the unconditional (actual) estimates of $\tilde{x}_{K,R}$and $\tilde{x}_{K,I}$ as follows:

(m, n)= $\arg min_{m,n} M^{\text{MAP}}\left(m, n, \tilde{X}_{K,R}^{(m,n)}, \tilde{X}_{K,I}^{(m,n)}\right)$,

Where $\tilde{X}_{K,R}^{(MAP)} = \tilde{X}_{K,R}^{(m,n)}$, $\tilde{X}_{K,I}^{(MAP)} = \tilde{X}_{K,I}^{(m,n)}$ (3.21)

To put it another way, after calculating the MAP estimates of $\tilde{x}_{K,R}$ and $\tilde{x}_{K,I}$ for every (m, n) ∈{ (1, 3), (1, 4), (2, 3), (2, 4), (3,5), (3,6), (4,7), (4,8)} that considers all active LD scenarios. The MIMO -OFDM scheme's conditional MAP estimator selects the most likely active LD pair $(\hat{m},\hat{n})$ and corresponding estimates of $\tilde{x}_{K,R}$and $\tilde{x}_{K,I}$ $\left(\tilde{X}_{K,R}^{(MAP)}, \tilde{X}_{K,I}^{(MAP)}\right)$ calculate the MAP estimate measure Eq. (3.17) for each of the four situations.

The following steps summarizes the steps of the proposed MAP estimator Algorithm.

1: for m = 1 : 2 : 3 : 4 do

2: for n = 3 : 4 : 5 : 6 do

3: Estimate, $\tilde{X}_{K,R}^{(m,n)}$ and $\tilde{X}_{K,I}^{(m,n)}$ values from (3.20)

4: Estimate, $(\acute{m}, \acute{n})$ indices from (3.21)

5: end for

6: end for

7: Combination of symbols: $\pm\tilde{X}_{K,R}^{(m,n)} \pm j\, \tilde{X}_{K,I}^{(m,n)}$ via $(\acute{m}, \acute{n})$.

The Ƕ/ξ The estimation of the complex OFDM signal xk is then calculated by the combiner.

$$\tilde{x}_{K,R} = \begin{cases} \tilde{X}_{K,R}^{(MAP)} & , \quad if \ m = 1,2,3 \\ -\tilde{X}_{K,R}^{(MAP)} & , \quad if \ m = 4 \end{cases} \tag{3.22}$$

$$\tilde{x}_{K,I} = \begin{cases} \tilde{X}_{K,I}^{(MAP)} & , \quad if \ m = 5,6,7 \\ -\tilde{X}_{K,I}^{(MAP)} & , \quad if \ m = 8 \end{cases}$$

Following this, traditional OFDM processing processes such as serial-to-parallel (S/P) conversion, FFT, and M-ary demodulation are used to generate an estimate $\acute{u}$ of the signal. the information bit vector u.

3.3.3 Calculation of Mean Square Error (MSE)

Given the estimates$(\acute{m},\acute{n})$ of the indices of the active LDs for k = 0, 1, · · · , N – 1, the mean-square error (MSE) is calculated for the estimations of q = $[\tilde{x}_{K,R} \ \tilde{x}_{K,I}]^T$ [65].

$$\text{MSE}_{y,q} = E\{\varepsilon^T \varepsilon\} \tag{3.23}$$

where ε represents the error vector, $\varepsilon = q - \acute{q}^{(\hat{m},\hat{n})}$ and $\acute{q} \equiv \acute{q}^{(\hat{m},\hat{n})} = [\tilde{x}_{K,R} \ \tilde{x}_{K,I}]^T$. As shown in Eqs. (3.13) and (3.20), $\acute{q}$ is linearly dependent on y, and the elements of $\acute{q}$ are jointly Gaussian distributed. As a result, ε is also Gaussian with zero mean, with the covariance matrix [67]:

$$\mathbf{C}^{(\hat{m},\hat{n})} = \left(\frac{1}{\sigma_q^2} I + \frac{1}{\sigma_n^2} H^T\right)^{-1} \in \mathrm{R}^{8\times 1} \tag{3.24}$$

where $\acute{H} = (h_{\acute{m}} \ h_{\acute{n}}) \in \mathrm{R}^{nR\times 1}$ and $\sigma_q^2 = \sigma_{\tilde{x}_{K,R(I)}}^2$ is the preceding density's variance of $\tilde{x}_{K,R(I)}$

It is easy to see fromEq. (3.14) that $\sigma_q^2 = \frac{\pi-1}{8\pi}$. Finally, for $k = 0, 1, \cdots, N-1$, The estimates' mean square error (MSE), $\tilde{X}_{K,R}^{(m,n)}$ and $\tilde{X}_{K,I}^{(m,n)}$ are equivalent to the error covariance matrix's diagonal members, namely,

$$\text{MSE}\left(\tilde{X}_{K,R}^{(m,n)}\right) = [\mathbf{C}^{(\hat{m},\hat{n})}]_{1,1}$$

$$\text{MSE}\left(\tilde{X}_{K,I}^{(m,n)}\right) = [\mathbf{C}^{(\hat{m},\hat{n})}]_{2,2} \quad (3.25)$$

Finally the average MSE for $\tilde{x}_{R(I)} = [\ \tilde{x}_{0,R(I)},\ \tilde{x}_{1,R(I)},\ \ldots\ ,\ \tilde{x}_{0,R(I)}\ ]^T$ can be obtained in the following manner:

$$\overline{\text{MSE}}\left(\tilde{x}_{R(I),}\right) = \frac{1}{\text{N}} \sum_{K=0}^{N-1} \text{MSE}\ \left(\tilde{X}_{K,R(I)}^{(m,n)}\right) \quad (3.26)$$

Table 3.2, it shows all the parameters that were used in the second section of this work.

Table 3.2 MIMO-Optical VLC parameters

Parameters	**Values**
Dimentions of the	6m × 6m × 3m
the total number of luminaries	8 × 8
the Number of LD Chips	64
Power of LD Chips	0.002 W
Luminary's viewing angle	120°
PD's FOV semi-angle (Degrees)	85°
PD area	1 cm^2

CHAPTER FOUR

Results and Discussion

4.1 Results and Discussion

This chapter gives results obtained from the proposed system using Matlab software and a detailed discussion for them.

4.2 Laser VLC System and Room Setup

In this section, a simulation is performed using the MATLAB software to verify the system performance for power and receiving SNRs. Three red, green, and blue (RGB) colors and nine recipient sites with a height of 1 m are tested. In addition, used the RGB colors system for transferring high data which is not considered for illuminate of room. In an empty room of 6m x 6m x 3m dimensions of (width x length x height), the room lighting is provided by five RGB-LD lighting units distributed in regular shapes where the LD lamps are installed 3m above the floor. As in Figure 3.1.

Table 4.1 shows the highest received power for the nine sites tested with an indication of the LDs received from it. Figure 4.1 displays the highest value of the SNR received for the tested sites with and without the reflector using the blue color.

Table 4.1: The PLOS & PFST in state of the position for blue color

N0	Position(meter) X	Y	Z	P_{LOS} (w)	P_{FST} (w)
1	1	1	1	LD_1 3.1663×10^{-13}	LD_1, LD_2 1.9159×10^{-12}
2	3	1	1	LD_1, LD_2 2.1920×10^{-13}	LD_1, LD_2 1.5844×10^{-12}
3	5	1	1	LD_2 3.1663×10^{-13}	LD_1, LD_2 6.2561×10^{-13}
4	1	3	1	LD_1, LD_3 2.1920×10^{-13}	LD_1, LD_2 9.4964×10^{-12}
5	3	3	1	LD_1, LD_2, LD_3, LD_4 1.6763×10^{-13}	LD_1, LD_2 5.3716×10^{-12}
6	5	3	1	LD_2, LD_4 2.1920×10^{-13}	LD_1, LD_2 9.8755×10^{-12}
7	1	5	1	LD_3 3.1663×10^{-13}	LD_1, LD_2 1.9159×10^{-12}
8	3	5	1	LD_3, LD_4 2.1920×10^{-13}	LD_1, LD_2 1.5844×10^{-12}
9	5	5	1	LD_4 3.1663×10^{-13}	LD_1, LD_2 6.2561×10^{-13}

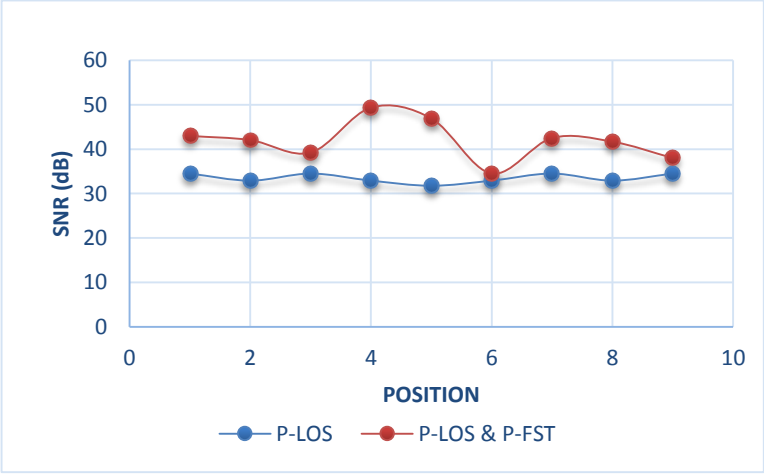

Figure 4.1: SNR versus test positions using P_{LOS} & (P_{LOS} & P_{FST}) for blue color

Table 4.2 provides the highest received power for the nine sites tested with an indication of the LD received from it. Figure 4.2 reveals the highest value of the SNR received for the tested sites with and without the reflector using the green color.

Table 4.2: Show PLOS & PFST in state of the position for green color

N0.	**Position(meter)** X	Y	Z	**PLOS (w)**	**PFST (w)**
1	1	1	1	LD_1 3.6588×10^{-13}	LD_1, LD_2 1.9159×10^{-12}
2	3	1	1	LD_1, LD_2 2.5330×10^{-13}	LD_1, LD_2 1.5844×10^{-12}
3	5	1	1	LD_2 3.6588×10^{-13}	LD_1, LD_2 6.2561×10^{-13}
4	1	3	1	LD_1, LD_3 2.5330×10^{-13}	LD_1, LD_2 9.4964×10^{-12}
5	3	3	1	LD_1, LD_2, LD_3, LD_4 1.9370×10^{-13}	LD_1, LD_2 5.3716×10^{-12}
6	5	3	1	LD_2, LD_4 2.5330×10^{-13}	LD_1, LD_2 9.8755×10^{-12}
7	1	5	1	LD_3 3.6588×10^{-13}	LD_1, LD_2 1.9159×10^{-12}
8	3	5	1	LD_3, LD_4 2.5330×10^{-13}	LD_1, LD_2 1.5844×10^{-12}
9	5	5	1	LD_4 3.6588×10^{-13}	LD_1, LD_2 6.2561×10^{-13}

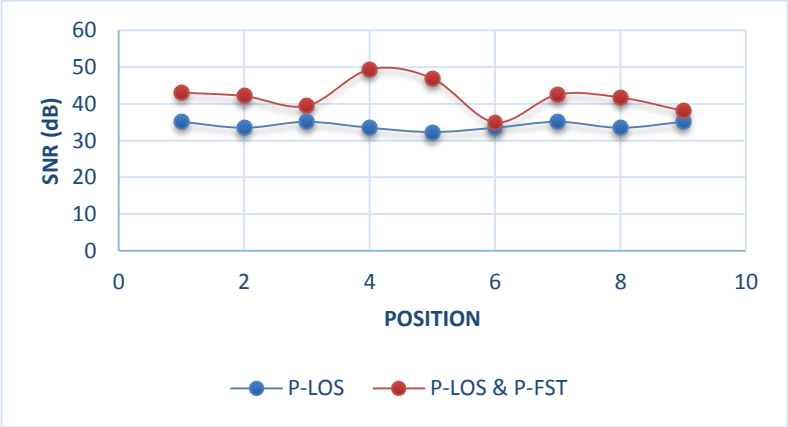

Figure 4.2: SNR versus test positions using P_{LOS} & (P_{LOS} & P_{FST}) for green color

Table 4.3 Shows the highest received power for the nine sites tested with an indication of the LD received from it. Figure 4.3 demonstrates the highest value of the SNR received for the tested sites with and without the reflector using the red color.

Table 4.3: Show PLOS & PFST in state of the position for red color

N0.	**Position(meter)** X	Y	Z	**P_{LOS} (w)**	**P_{FST} (w)**
1	1	1	1	LD_1 4.4680×10^{-13}	LD_1,LD_2 1.9159×10^{-12}
2	3	1	1	LD_1,LD_2 3.0932×10^{-13}	LD_1,LD_2 1.5844×10^{-12}
3	5	1	1	LD_2 4.4680×10^{-13}	LD_1,LD_2 6.2561×10^{-13}
4	1	3	1	LD_1,LD_3 3.0932×10^{-13}	LD_1,LD_2 9.4964×10^{-12}
5	3	3	1	LD_1,LD_2,LD_3,LD_4 2.3654×10^{-13}	LD_1,LD_2 5.3716×10^{-12}
6	5	3	1	LD_2,LD_4 3.0932×10^{-13}	LD_1,LD_2 9.8755×10^{-12}
7	1	5	1	LD_3 4.4680×10^{-13}	LD_1,LD_2 1.9159×10^{-12}
8	3	5	1	LD_3,LD_4 3.0932×10^{-13}	LD_1,LD_2 1.5844×10^{-12}
9	5	5	1	LD_4 4.4680×10^{-13}	LD_1,LD_2 6.2561×10^{-13}

Figure 4.3: SNR versus test positions using P_{LOS} & (P_{LOS} & P_{FST}) for red color

As obtained from the previous results, it can be observed that in the presence of the inverter, the SNR value of the three tested colors has increased by increasing the received power, and the highest SNR value of (50 dB) for the colors (RGB) is obtained at position 4 Through sources (LD1, LD3) and the lowest SNR value is (34 dB) for colors (RGB) at position 6 through sources (LD2, LD4).

4.3 Generalized LD Index Modulation with Optical MIMO-OFDM

The approach for obtaining physical multi path VLC channels is described in this section. Humans in the room, the frame of furniture, including types of coating materials, object location, and sources/detectors all have an impact on reflection and refraction patterns. For higher order reflections, all of these physical features are taken into consideration.

To analyse the frequency elective visible light channel models, we have used IEEE 802.15.7r1 reference channel models that are obtained for manufacturing cells. Eight LDs are situated at the ceiling of the room. Each LD has one transmitter, providing 360-degree coverage. The detector's area and the semi-angle of the FOV, respectively, are 1 cm^2 and 35cm^2. At the top of the cell boundaries, eight test points are also taken into account. We choose the LD_1- LD_8 as transmitters and D_1-D_8 as receivers (i.e., positioned at the cell borders' corners). Because of the VLC channels' different delays under test and signaling rates of more than 100 Mbits/sec, the multipath components are resolvable, and they can be thought of as multitap channels that lead to frequency selective channels.

For more consideration, the channel's sample frequency f_s is set to 100 MHz, with a sampling time of Ts = 10 ns. Down sampling L = 4 taps frequency selective VLC channel vectors are used because the resultant channel's maximum delay spread is 60 ns.

4.4 Analytical Channel Gain

To put into action the conditional MAP technique for an estimate of the real channel route gain for the MIMO-OFDM receiver, only C and D must be computed in Eq. (3.21) . A, B, and E can be computed ahead of time and saved in the receiver because the channel is stable and does not vary over time. As a result, 8 x 8 N real multiplications (RM) and 64N real additions (RA) are required for all (m, n) pairs where m = 1,2,3,4 and n = 5, 6,7,8 for k = 1, 2, • • •, N values. In addition, 32N RM and 16N RA are required for the MAP metric to be computed in order to calculate the indices of the active LDs. The OFDM technique, on the other hand, needs roughly 8N log2(N) real operations with an FFT size of N (multiplications plus additions).

$$H1=\begin{bmatrix} 0.600 & 0.480 & 0.528 & 0.460 & 0.456 & 0.412 & 0.384 & 0.352 \\ 0.480 & 0.600 & 0.460 & 0.528 & 0.412 & 0.456 & 0.352 & 0.384 \\ 0.528 & 0.460 & 0.600 & 0.480 & 0.528 & 0.460 & 0.456 & 0.412 \\ 0.460 & 0.528 & 0.480 & 0.600 & 0.460 & 0.528 & 0.412 & 0.456 \\ 0.456 & 0.412 & 0.528 & 0.460 & 0.600 & 0.480 & 0.528 & 0.460 \\ 0.412 & 0.465 & 0.460 & 0.528 & 0.480 & 0.600 & 0.460 & 0.528 \\ 0.384 & 0.352 & 0.456 & 0.412 & 0.528 & 0.460 & 0.600 & 0.480 \\ 0.352 & 0.384 & 0.412 & 0.456 & 0.460 & 0.528 & 0.480 & 0.600 \end{bmatrix}$$

$$H2=\begin{bmatrix} 0.480 & 0.600 & 0.460 & 0.528 & 0.412 & 0.456 & 0.352 & 0.384 \\ 0.600 & 0.480 & 0.528 & 0.460 & 0.456 & 0.412 & 0.384 & 0.352 \\ 0.528 & 0.460 & 0.600 & 0.480 & 0.528 & 0.460 & 0.456 & 0.412 \\ 0.460 & 0.528 & 0.480 & 0.600 & 0.460 & 0.528 & 0.412 & 0.456 \\ 0.456 & 0.412 & 0.528 & 0.460 & 0.600 & 0.480 & 0.528 & 0.460 \\ 0.412 & 0.465 & 0.460 & 0.528 & 0.480 & 0.600 & 0.460 & 0.528 \\ 0.384 & 0.352 & 0.456 & 0.412 & 0.528 & 0.460 & 0.600 & 0.480 \\ 0.352 & 0.384 & 0.412 & 0.456 & 0.460 & 0.528 & 0.480 & 0.600 \end{bmatrix}$$

$$H3=\begin{bmatrix}0.528 & 0.460 & 0.600 & 0.480 & 0.528 & 0.460 & 0.456 & 0.412\\ 0.600 & 0.480 & 0.528 & 0.460 & 0.456 & 0.412 & 0.384 & 0.352\\ 0.480 & 0.600 & 0.460 & 0.528 & 0.412 & 0.456 & 0.352 & 0.384\\ 0.460 & 0.528 & 0.480 & 0.600 & 0.460 & 0.528 & 0.412 & 0.456\\ 0.456 & 0.412 & 0.528 & 0.460 & 0.600 & 0.480 & 0.528 & 0.460\\ 0.412 & 0.465 & 0.460 & 0.528 & 0.480 & 0.600 & 0.460 & 0.528\\ 0.384 & 0.352 & 0.456 & 0.412 & 0.528 & 0.460 & 0.600 & 0.480\\ 0.352 & 0.384 & 0.412 & 0.456 & 0.460 & 0.528 & 0.480 & 0.600\end{bmatrix}$$

$$H4=\begin{bmatrix}0.460 & 0.528 & 0.480 & 0.600 & 0.460 & 0.528 & 0.412 & 0.456\\ 0.600 & 0.480 & 0.528 & 0.460 & 0.456 & 0.412 & 0.384 & 0.352\\ 0.480 & 0.600 & 0.460 & 0.528 & 0.412 & 0.456 & 0.352 & 0.384\\ 0.528 & 0.460 & 0.600 & 0.480 & 0.528 & 0.460 & 0.456 & 0.412\\ 0.456 & 0.412 & 0.528 & 0.460 & 0.600 & 0.480 & 0.528 & 0.460\\ 0.412 & 0.465 & 0.460 & 0.528 & 0.480 & 0.600 & 0.460 & 0.528\\ 0.384 & 0.352 & 0.456 & 0.412 & 0.528 & 0.460 & 0.600 & 0.480\\ 0.352 & 0.384 & 0.412 & 0.456 & 0.460 & 0.528 & 0.480 & 0.600\end{bmatrix}$$

$$H5=\begin{bmatrix}0.456 & 0.412 & 0.528 & 0.460 & 0.600 & 0.480 & 0.528 & 0.460\\ 0.600 & 0.480 & 0.528 & 0.460 & 0.456 & 0.412 & 0.384 & 0.352\\ 0.480 & 0.600 & 0.460 & 0.528 & 0.412 & 0.456 & 0.352 & 0.384\\ 0.528 & 0.460 & 0.600 & 0.480 & 0.528 & 0.460 & 0.456 & 0.412\\ 0.460 & 0.528 & 0.480 & 0.600 & 0.460 & 0.528 & 0.412 & 0.456\\ 0.412 & 0.456 & 0.460 & 0.528 & 0.480 & 0.600 & 0.460 & 0.528\\ 0.384 & 0.352 & 0.456 & 0.412 & 0.528 & 0.460 & 0.600 & 0.480\\ 0.352 & 0.384 & 0.412 & 0.456 & 0.460 & 0.528 & 0.480 & 0.600\end{bmatrix}$$

$$H6=\begin{bmatrix}0.412 & 0.456 & 0.460 & 0.528 & 0.480 & 0.600 & 0.460 & 0.528\\ 0.600 & 0.480 & 0.528 & 0.460 & 0.456 & 0.412 & 0.384 & 0.352\\ 0.480 & 0.600 & 0.460 & 0.528 & 0.412 & 0.456 & 0.352 & 0.384\\ 0.528 & 0.460 & 0.600 & 0.480 & 0.528 & 0.460 & 0.456 & 0.412\\ 0.460 & 0.528 & 0.480 & 0.600 & 0.460 & 0.528 & 0.412 & 0.456\\ 0.456 & 0.412 & 0.528 & 0.460 & 0.600 & 0.480 & 0.528 & 0.460\\ 0.384 & 0.352 & 0.456 & 0.412 & 0.528 & 0.460 & 0.600 & 0.480\\ 0.352 & 0.384 & 0.412 & 0.456 & 0.460 & 0.528 & 0.480 & 0.600\end{bmatrix}$$

$$H7=\begin{bmatrix}0.384 & 0.352 & 0.456 & 0.412 & 0.528 & 0.460 & 0.600 & 0.480\\ 0.600 & 0.480 & 0.528 & 0.460 & 0.456 & 0.412 & 0.384 & 0.352\\ 0.480 & 0.600 & 0.460 & 0.528 & 0.412 & 0.456 & 0.352 & 0.384\\ 0.528 & 0.460 & 0.600 & 0.480 & 0.528 & 0.460 & 0.456 & 0.412\\ 0.460 & 0.528 & 0.480 & 0.600 & 0.460 & 0.528 & 0.412 & 0.456\\ 0.456 & 0.412 & 0.528 & 0.460 & 0.600 & 0.480 & 0.528 & 0.460\\ 0.412 & 0.456 & 0.460 & 0.528 & 0.480 & 0.600 & 0.460 & 0.528\\ 0.352 & 0.384 & 0.412 & 0.456 & 0.460 & 0.528 & 0.480 & 0.600\end{bmatrix}$$

$$H8=\begin{bmatrix} 0.352 & 0.384 & 0.412 & 0.456 & 0.460 & 0.528 & 0.480 & 0.600 \\ 0.600 & 0.480 & 0.528 & 0.460 & 0.456 & 0.412 & 0.384 & 0.352 \\ 0.480 & 0.600 & 0.460 & 0.528 & 0.412 & 0.456 & 0.452 & 0.384 \\ 0.528 & 0.460 & 0.600 & 0.480 & 0.528 & 0.460 & 0.456 & 0.412 \\ 0.460 & 0.528 & 0.480 & 0.600 & 0.460 & 0.528 & 0.412 & 0.456 \\ 0.456 & 0.412 & 0.528 & 0.460 & 0.600 & 0.480 & 0.528 & 0.460 \\ 0.412 & 0.456 & 0.460 & 0.528 & 0.480 & 0.600 & 0.460 & 0.528 \\ 0.384 & 0.352 & 0.456 & 0.412 & 0.528 & 0.460 & 0.600 & 0.480 \end{bmatrix}$$

4.5 Performance of MIMO -OFDM

In this section, the BER performance of the MIMO-OFDM scheme to that of the reference systems in terms of average received electrical SNR is compared. In the analyses, several VLC channel configurations, demonstrate BER versus SNR performance curves for spectral efficiency values of 1, 2, 3, and 4 bit/sec/Hz., with N = 256 subcarriers.

In Figures 4.9 and 4.11, the suggested system's BER performance is compared to that of various reference MIMO systems. These graphs indicate that the MIMO-OFDM outperforms the other reference systems in Figure 4.9, however, the curve in Figure 4.11 shows that this is not. For the rest of the curves, Figures 4.5, 4.6, 4.7, 4.8, 4.10, 4.12, one can see a note that they are at a moderate or fairly acceptable level. This can be explained that the BER performance of the MIMO-OFDM system is heavily influenced by the relationship between diagonal (LOS/direct) and off-diagonal (NLOS/indirect) parts of the channel matrix. When the channel matrix is close to the diagonal, it provides great BER performance. To assess how being “close” to the diagonal affects the channel matrix

entries, a reasonable technique is to calculate the correlation coefficient between the columns and rows of the channel matrix. Strong correlation indicates that the matrix elements are centered on the diagonal and that is close to one. This is also resilient because when the channel matrix is scaled, the correlation coefficient remains unchanged. However, the channel matrices of the various configurations evaluated can be divided into eight different channel topologies based on the correlation values. As a result, H_6 and H_7 have the lowest correlation values and are hence the furthest from a diagonal matrix structure. H_1, H_2, H_3, H_4 and H_8, on the other hand, have a mild diagonal structure, whereas H_5, the last channel matrix, has a substantial diagonal structure.

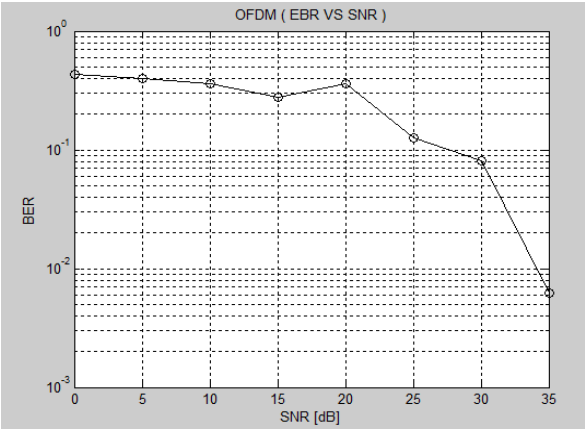

Fig. 4.5. Optical MIMO-OFDM performance BER comparison scheme in analytic channel H1

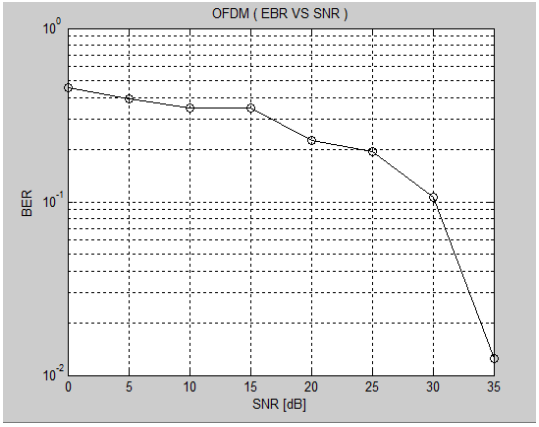

Fig. 4.6. Optical MIMO-OFDM performance BER comparison scheme in analytic channel H2

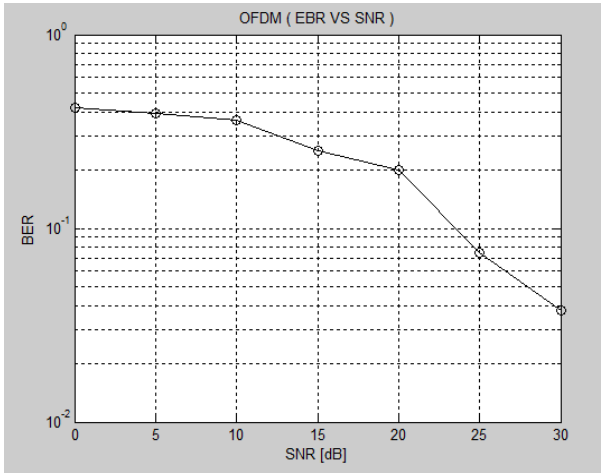

Fig. 4.7. Optical MIMO-OFDM performance BER comparison scheme in analytic channel H3

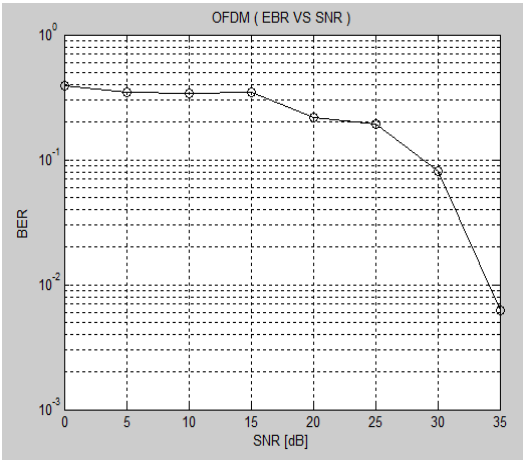

Fig. 4.8. Optical MIMO-OFDM performance BER comparison scheme in analytic channel H4

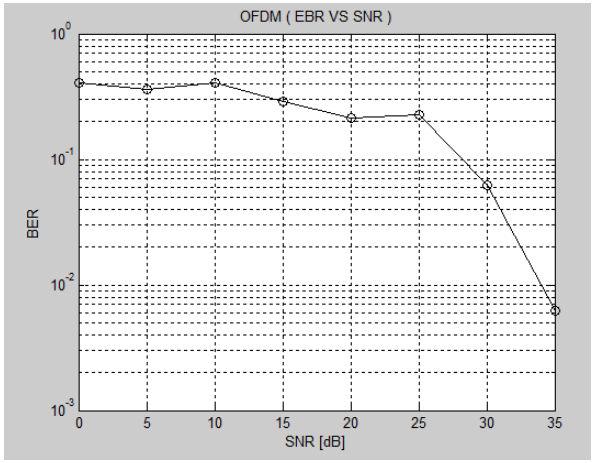

Fig. 4.9. Optical MIMO-OFDM performance BER comparison scheme in analytic channel H5

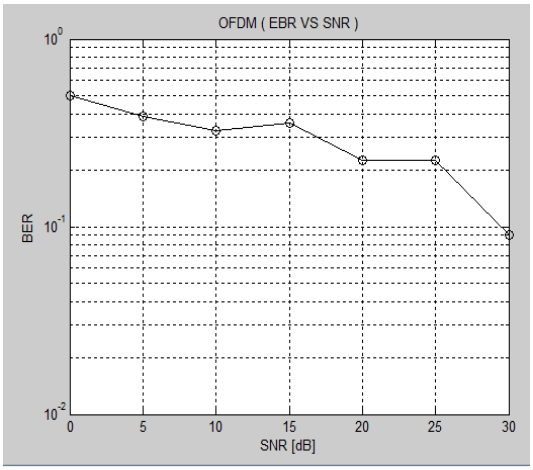

Fig. 4.10. Optical MIMO-OFDM performance BER comparison scheme in analytic channel H6

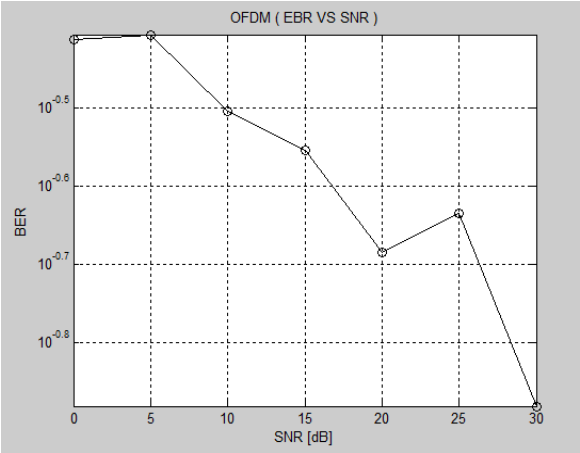

Fig. 4.11. Optical MIMO-OFDM performance BER comparison scheme in analytic channel H7

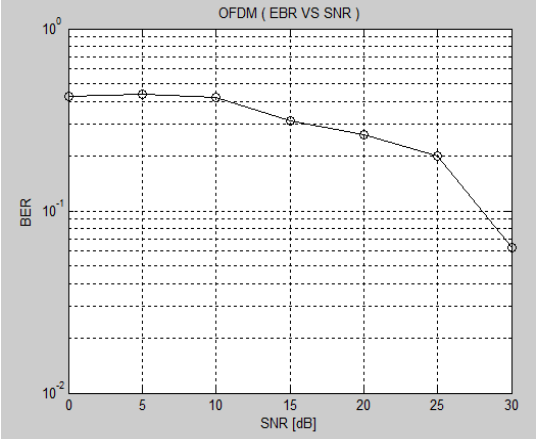

Fig. 4.12. Optical MIMO-OFDM performance BER comparison scheme in analytic channel H8

Finally, using both physical and analytical channel matrices, MSE and SNR curve for MIMO -OFDM are shown in Figure 4.13. Furthermore, the theoretic MSE values are compared to the outcomes of computer simulations. The theoretic and computer simulation curve correspond very well, especially at high SNR levels.

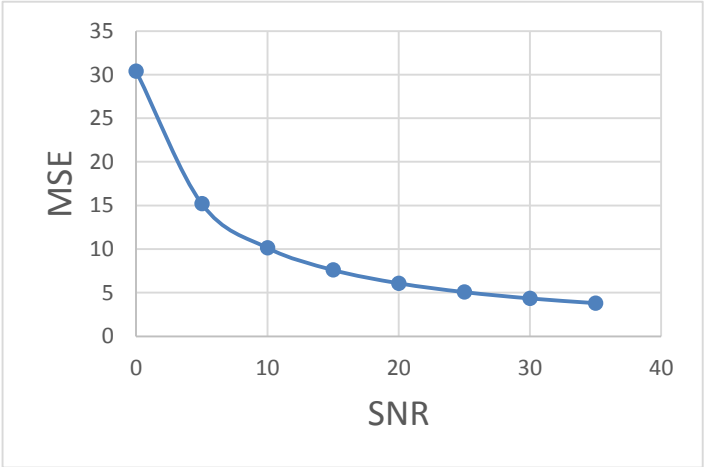

Figure 4.13. An simulated and analytical MSE comparison for analytic channels

CHAPTER FIVE

Conclusions and Future Works

The most essential goals of this thesis will be discussed, as well as the conclusions obtained from each design. After that, underline the most important recommendations.

5.1 Conclusions

Visible light communication (VLC) systems have become promising candidates to complement conventional radio frequency (RF) systems due to the increasingly saturated RF band and the potentially high data rates that can be achieved by VLC systems. The maximum value of the Signal-to-Noise Ratio (SNR) is (50 dB) in the fourth position through sources, according to the above-mentioned systems (LD1, LD3). The lowest result (34 dB) in the sixth place is obtained from sources (LD2, LD4), which is relevant to the initial segment of this study (Positioning and reflected algorithm). The highest value of SNR is (35 dB) when BER (0.0082 vs) is in channel 5 at location (8,7), and the lowest value is (30 dB) when the BER ($10^{-0.9}$ vs) is in channel 7 at location (8), according to the second half of this work. Finally, the MSE against SNR curves for MIMO-OFDM are given utilizing both analyte and physical channel matrices. The outcomes of computer simulations are compared to the theoretical values of tiny problems. Particularly at high SNR levels, the theoretical and computer simulation curves fit quite well.

5.2 Recommendations for future work

Work on visible light communications in multiple locations and multiple input multiplexing has been done in this study. Moreover, there are a number of topics that should be researched in the future.

1) Carry out this work in practice.

2) Design and analysis of GPS Visible Light Communications (VLC) based on the use of multiple reflectors.

3) Design and analysis of the positioning of visible light communications (VLC) based on code division multiple access (CDMA).

4) Design and analysis of positioning for visible light communications (VLC) based on the Hadamard encoded modification (HCM).

5) Design and analysis of multiple-input, multiple-output MIMO for visual-light communication with LD positioning arrangement and considering the effect of walls, furniture, shading and sunlight.

REFERENCES

[1] H. H. Dobroslav Tsonev, Stefan Videv, “Light Fidelity (Li-Fi): Towards All-Optical Networking,” in Proc. SPIE 9007, *Broadband Access Communication Technologies VIII*, 900702, vol. 9007, 2014.

[2] Cisco Visual Networking Index: Global Mobile Data Traffic Forecast Update, 2015–2020 White Paper, [online]: http://www.cisco.com/c/en/us/solutions/collateral/serviceprovider/ visual-networking-index-vni/white_paper_c11-520862.html.

[3] WiGig and Wi-Fi Alliance, [online]: http://www.wi-fi.org/discover-wi-fi/wigig-certified.

[4] D. O'Brien, G. Parry, and P. Stavrinou, "Optical hotspots speed up wireless communication," *Nature Photonics*, vol.1, no.5, pp.245-247, 2007.

[5] F. R. Gfeller, and U. Bapst, "Wireless in-house data communication via diffuse infrared radiation," *Proceedings of the IEEE*, vol. 67, no.11, pp.1474-1486, 1979.

[6] G. Yun and M. Kavehrad, "Spot-diffusing and fly-eye receivers for indoor infrared wireless communications," *IEEE International Conference on Selected Topics in Wireless Communications*, pp.262-265, 1992.

[7] M. D. Audeh and J. M. Kahn, "Performance evaluation of baseband OOK for wireless indoor infrared LAN's operating at 100 Mb/s," *IEEE Transactions on Communications*, vol. 43, issue 6, pp.2085-2094, 1995.

[8] A. G. Al-Ghamdi, and J. M. H. Elmirghani, "Performance evaluation of a triangular pyramidal fly-eye diversity detector for optical wireless communications," *IEEE Communications Magazine*, vol. 41, issue 3, pp.80-86, 2003.

[9] M. Kavehrad, and S. Jivkova, "Indoor broadband optical wireless communications: optical subsystems designs and their impact on channel characteristics," *IEEE Wireless Communications*, vol.10, issue 2, pp.30-35, 2003.

[10] O. Gonzalez, R. Perez-Jimenez, S. Rodriguez, J. Rabadan, and A. Ayala, "OFDM over indoor wireless optical channel," *IEEE Proceedings Optoelectronics*, vol. 52, issue 4, pp.199-204, 2005.

[11] Z. Ghassemlooy, W. Popoola, and S. Rajbhandari, "Optical wireless communications: system and channel modelling with MATLAB," *CRC Press*, 2012.

[12] J. M. Kahn, and J. R. Barry, "Wireless infrared communications," *Proceedings of the IEEE*, vol.85, issue 2, pp.265-298, 1997.

[13] J. M. Kahn, J. Barry, W. Krause, M. Audeh, J. Carruthers, and G. Marsh, "High-speed non-directional infrared communication for wireless local-area networks," *Twenty-Sixth Asilomar Conference on Signals, Systems and Computers*, pp. 83-87, 1992.

[14] T. Komine and M. Nakagawa, "Fundamental analysis for visible-light communication system using LED lights" *IEEE Transactions on Consumer Electronics*, vol. 50, issue 1, pp.100-107, 2004.

[15] Energy Efficiency of White LEDs, [online]: http://www.fcgov.com /utilities/img/site_specific/uploads/led-efficiency.pdf

[16] Ahmed Taha Hussein, " Visible Light Communication System," December 2016.

[17] S. Haruyama, "Visible light communications: Recent activities in Japan," *A Smart Lighting ERC Industry—Academia Day at BU Photonics Center, Boston University, 2011.*

[18] M. Nakajima, and S. Haruyama, "New indoor navigation system for visually impaired people using visible light communication," *EURASIP Journal on Wireless Communications and Networking*, vol.1, no.1, pp.1-10, 2013.

[19] K. Panta, and J. Armstrong, "Indoor localisation using white LEDs," *Electronics letters*, vol.48, issue 4, pp.228-230, 2012.

[20] S. Y. Jung, S. Hann, and C.-S. Park, "TDOA-based optical wireless indoor localization using LED ceiling lamps," *IEEE Transactions on Consumer Electronics*, vol.57, issue 4, pp.1592-1597, 2011.

[21] W. Zhang, and M. Kavehrad, "Comparison of VLC-based indoor positioning techniques," *SPIE Proceedings*, vol.8645, no.1, pp.86450M-86450M-6, 2013.

[22] H. Binti Che Wook, T. Komine, S. Haruyama, and M. Nakagawa, "Visible light communication with LED-based traffic lights using 2-dimensional image sensor," *3rd IEEE in Consumer Communications and Networking Conference*, pp.243-247, 2006.

[23] A. T. Hussein, and J. M. H. Elmirghani, "A Survey of Optical and Terahertz (THz) Wireless Communication Systems," *IEEE Communications Surveys & Tutorials*, (to be submitted), 2016.

[24] X. Ning, R. Winston, and J. O'Gallagher, "Dielectric totally internally reflecting concentrators," *Applied Optics*, vol. 26, no.1, pp.300-305, 1987.

[25] J. P. Savicki and S. P. Morgan, "Hemispherical concentrators and spectral filters for planar sensors in diffuse radiation fields," *Applied optics*, vol.33, no.1, pp.8057-8061,1994.

[26] K. P. Ho and J. M. Kahn, "Compound parabolic concentrators for narrowband wireless infrared receivers," *Optical Engineering*, vol.34, issue 5, pp.1385-1395, 1995.

[27] J. Fadlullah and M. Kavehrad, "Indoor high-bandwidth optical wireless links for sensor networks," *Journal of lightwave technology*, vol.28, issue 21, pp.3086-3094, 2010.

[28] S. Arnon, "Visible light communication, " *Cambridge University Press*, 2015.

[29] Getting to Know LEDs and Solutions, [online]: http://www.dialight.com /Assets%5CApplication_Notes%5CIndication%5CGetting%20To%20Know%20LEDs. PDF.

[30] K. Asatani, and T. Kimura, "Analyses of LED nonlinear distortions," *IEEE Journal of Solid-State Circuits*, vol.13, issue 1, pp.125-133, 1978.

[31] K. Lee, H. Park, and J. R. Barry, "Indoor channel characteristics for visible light communications," *IEEE Communications Letters*, vol.15, issue 2, pp.217-219, 2011.

[32] J. R. Barry and J. M. Kahn, "Link design for nondirected wireless infrared communications," *Applied optics*, vol.34, no.19, pp.3764-3776, 1995.

[33] E. Sarbazi, M. Uysal, M. Abdallah, and K. Qaraqe, "Indoor channel modelling and characterization for visible light communications," *International Conference in Transparent Optical Networks (ICTON 2014)*, pp.1-4, 2014.

[34] A. J. Moreira, R. T. Valadas, and A. de Oliveira Duarte, "Optical interference produced by artificial light," *Wireless Networks*, vol.3, issue 6, pp.131-140, 1997.

[35] A. J. Moreira, R. T. Valadas, and A. de Oliveira Duarte, "Characterisation and modelling of artificial light interference in optical wireless communication systems," *IEEE International Symposium in Personal, Indoor and Mobile Radio Communications*, pp.326-331, 1995.

[36] A. J. Moreira, R. T. Valadas, and A. de Oliveira Duarte, "Reducing the effects of artificial light interference in wireless infrared transmission systems," *IEEE Colloquium Optical Free Space Communication Links*, pp.1-5, 1996.

[37] L.-M. Hoa, D. O'Brien, G. Faulkner, Z. Lubin, L. Kyungwoo, and J. Daekwang, "100-Mb/s NRZ Visible Light Communications Using a Postequalized White LED," *IEEE Photonics Technology Letters*, vol.21, issue 15, pp.1063-1065, 2009.

[38] D. O'Brien, L. Zeng, L.-M. Hoa, G. Faulkner, J. W. Walewski, and S. Randel, "Visible light communications: Challenges and possibilities," *IEEE 19th International Symposium in Personal, Indoor and Mobile Radio Communications*, pp.1-5, 2008.

[39] A. Street, P. Stavrinou, D. O'brien, and D. Edwards, "Indoor optical wireless systems–a review," *Optical and Quantum Electronics*, vol.29, issue 3, pp.349-378, 1997.

[40] A. Boucouvalas, "Indoor ambient light noise and its effect on wireless optical links," *IEEE Proceedings Optoelectronics*, vol.143, issue 6, pp.334-338, 1996.

[41] A. J. C. Moreira, R. T. Valadas, and A. M. de Oliveira Duarte, "Performance of infrared transmission systems under ambient light interference," *IEEE Proceedings Optoelectronics*, vol.143, issue 6, pp.339-346, 1996.

[42] J. M. H. Elmirghani, H. H. Chan, and R. A. Cryan, "Sensitivity evaluation of optical wireless PPM systems utilising PIN-BJT receivers," *IEEE Proceedings Optoelectronics*, vol.143, issue 6, pp.355-359, 1996.

[43] JEITA, "CP-1221 Visible Light Communications System,", 2007.

[44] JEITA, "CP-1222 Visible Light ID System,", 2007.

[45] OMEGA Project, [online]: http://www.ict-omega.eu/home.html.

[46] Smart Lighting, [online]: http://smartlighting.rpi.edu/index.shtml.

[47] "IEEE Standard for Local and Metropolitan Area Networks--Part 15.7: Short-Range Wireless Optical Communication Using Visible Light," *IEEE Std 802.15.7-2011*, pp.1-309, 2011.

[48] SAIF SAAD HAMEED, ARUN KUMAR SHUKLA, "Design and Analysis Optical Wireless Communication Based on “Li-Fi”," *International Journal of Scientific Engineering and Technology Research*, vol. 03, issue 03, pp. 0491-0494, 2014.

[49] Huichao Lv,Lihui Feng,Aiying Yang,Peng Guo,Heqing Huang, Shufen Chen, "High Accuracy VLC Indoor Positioning System With Differential Detection," *IEEE Photonics Journal*, vol. 9, Number 3, 2017.

[50] Thomas Little, Michael Rahaim, Iman Abdalla, Emily Lam, Richard Mcallister, Anna Maria Vegni, "A Multi-Cell Lighting Testbed for VLC and VLP," *Engineering Research Centers Pro- gram of the National Science Foundation under NSF Cooperative Agreemen No. EEC-0812056 and by NSF No. CNS-1617924*., 2018.

[51] Sheng Zhang, Pengfei Du, Chen Chen, and Wen-De Zhong, "3D Indoor Visible Light Positioning System using RSS ratio with Neural Network," *Conference Paper*, 2018.

[52] Imran Khan1, Haque Nawaz1, M. M. Rind1, Kamlesh Kumar1, M. A. Chahajro1, Abdullah Mailto2, " Comparative Study of Existing and Forthcoming WLAN Technologies," *IJCSNS International Journal of Computer Science and Network Security*, VOL.18 No.4, April 2018.

[53] Abdullah Ali Qasim, M.F.L. Abdullah, R.Talib, Hassan Muwafaq gheni, Khaldoon Anmar Omar, Anas Malik Abdulrahman, " Visible Light Communication the next Future Generation System," *International Conference on Information Science and Communication Technology (ICISCT)*, 2019

[54] Yinzhou Tan, Xiping Wu and Harald Haas, " Performance Comparison between Coherent and DCO-OFDM LiFi Systems," *IEEE*,2019

[55] Mohammed S.M. Gismalla1, Mohammad F.L. Abdullah1, Mussaab I. Niass2,Bhagwan Das3, Wafi A. Mabrouk1, " Improve uniformity for an indoor visible light communication system," *Int J Commun Syst.*,2019.

[56] Cătălin Beguni, Sebastian-Andrei Avătămăniței, Alin-Mihai Căilean, Eduard Zadobrischi,Mihai Dimian, Hongyu Guan and Luc Chassagne, " Toward a mixed visible light communications and ranging system for automotive applications " *IEEE*, 2019.

[57] Radek Martinek *, Lukas Danys *, Rene Jaros *, " Visible Light Communication System Based on Software Defined Radio: Performance Study of Intelligent Transportation and Indoor Applications," *Electronics*, 8,2019.

[58] Sathisha R N, Vidit Jha, Faheem Ahmad, Varun Raghunathan, " Demonstration of High Data-rate Multimedia Streaming in a Laser-based Indoor Visible Light Communication System," *12th International Conference on Communication Systems & Networks (COMSNETS)*, 2020.

[59] Saif N. Ismail1,a) and Muataz H. Salih2, " A Review of Visible Light Communication (VLC)Technology," *2nd International Conference on Materials Engineering & Science (IConMEAS 2019)*, 2020.

[60] European standard EN 12464-1: Lighting of indoor work places, 2003.

[61] A. Nuwanpriya, A. Grant, S.-W. Ho, and L. Luo, "Position modulating OFDM for optical wireless communications," *in Proc. IEEE Globecom Workshops, Anaheim, CA, USA, Dec*. 2012, pp. 1219—1223.

[62] Faris Mohammed Ali 1, Bashar J. Hamza2, Yassen H. Taher3, "Design and evaluation of optical laser diodes LD positioning arrangement and multiple input/ multiple output MIMO-OFDM systems Periodicals of Engineering and Natural Sciences. Vol. 8 , No. 3, pp.1345-1358, July 2020

[63] T. Fath, J. Klaue, and H. Haas, "Coded Spatial Modulation applied to Optical Wireless Communications in Indoor Environments," *in IEEE Proc. of the Wireless*

Communications and Networking Conference (WCNC). Paris, France: IEEE, Apr. 1–4 2012, pp. 1000 – 1004.

[64] F. Miramirkhani and M. Uysal, "Channel modeling and characterization for visible light communications," *IEEE Photon. J.*, vol. 7, no. 6, Dec. 2015.

[65] Anil Yesilkaya, Farshad Miramirkhani, Murat Uysal, " Optical MIMO-OFDM With Generalized LED Index Modulation," *IEEE TRANSACTIONS ON COMMUNICATIONS,* VOL. 65, NO. 8, AUGUST 2017

[66] Y. Li, D. Tsonev, and H. Haas, "Non-DC-biased OFDM with optical spatial modulation," *in Proc. IEEE 24th Ann. Int. Symp. Pers., Indoor, Mobile Radio Commun. (PIMRC), London, U.K.,* Sep. 2013, pp. 486—490.

[67] S. M. Kay, Fundamentals Statistical Signal Processing: Estimation Theory. Upper Saddle River, NJ, USA: Prentice-Hall, 1993.

LIST OF PUBLICATION

1. " Study and Evaluation of Different Link Configurations of Laser Diodes positioning for Line of Sight and Non-Line of Sight Ray Tracing" has been Published in Advances in Mechanics,which is scopus journal,2021.
2. "LD Index Modulation in Optical MIMO-OFDM with Frequency-Flat MIMO Channels and Conditional MAP Estimator ", submitted to the Al-Furat Journal of Innovations in Electronics and Computer Engineering (FJIECE).

الخلاصة

الاتصالات البصرية المرئية (VLC) هي تقنية جديدة واعدة وغير معروفة للجيل القادم من أنظمة الاتصالات اللاسلكية التي حسنت سرعة نقل البيانات. علاوة على ذلك ، تقنية الشبكات الضوئية اللاسلكية التي تستخدم الضوء المرئي كوسيلة لنقل البيانات لتقديم اتصال عالي السرعة في نظام الاتصالات - مثل أسلوب Wi-Fi (الدقة اللاسلكية). في هذه الأطروحة تقدم خوارزمية جديدة لنظام تحديد موقع الثنائي الضوئي بالليزر (LD) على أساس تتبع الشعاع في وضع الانعكاس من الدرجة الأولى. يستخدم نظام الاتصالات البصرية المرئية صمامات ليزر ثنائية (LDs) ، تتكون كل واحدة منها من مقاطع 5 × 5 LD. تم تقديم نموذج الانتشار متعدد المسارات وتقييم SNR في هذه الأطروحة.

بالإضافة إلى ذلك ، تم إجراء تقنية جديدة تعتمد على إرسال 8 × 8 MIMO يسمى MIMO- OFDM (مدخلات متعددة ومخرجات متعددة وتعدد الإرسال المتعامد بتقسيم التردد). في مخطط العمل ، يتم فصل الأجزاء الحقيقية والخيالية لإشارات OFDM المؤقتة المعقدة إلى أجزائها الحقيقية والخيالية ، ثم يتم إرسال هذه الإشارات عبر قناة MIMO-VLC باستخدام تعديل المؤشر على أساس المصابيح النشطة. يتم تحقيق كفاءات طيفية وطاقة أعلى عن طريق تشفير معلومات الإشارة المعقدة في موضع مصابيح LED للإرسال. علاوة على ذلك ، يتم استخدام مقدر الاحتمالية القصوى (MAP) لتقدير تلك الأجزاء الحقيقية والخيالية من إشارات OFDM في جهاز الاستقبال وكذلك تمت مقارنة متوسط الخطأ التربيعي (MSE) مع (SNR) وتم تصميمه ومحاكاته باستخدام برنامج MATLAB.
من خلال الأنظمة المذكورة أعلاه ، وجد أن أعلى قيمة لنسبة الإشارة إلى الضوضاء (SNR) كانت (50 dB) في الموقع الرابع من خلال المصادر (LD_1، LD_3). وأقل قيمة كانت (34 dB) في الموقع السادس من خلال المصادر (LD_2، LD_4) هذا بخصوص القسم الأول من هذا العمل (خوارزمية تحديد المواقع والانعكاس).

أما بالنسبة لـ (MIMO-OFDM with LD Index Modulation Optical) ، وهو القسم الثاني من هذا العمل ، فقد اتضح أن أعلى قيمة لـ SNR كانت (35 dB) عندما كان معدل الخطأ في البت (BER) أقل من 10^{-2}وهذا حوالي (0.0082) كان في القناة 5 في الموقع (8,7) وكانت أقل قيمة (30 dB) عند معدل خطأ البت (10^{-}) (BER

$^{0.9}$) في القناة 7 في الموقع (8) ، بينما متطلبات SNR المعترف بها عالميًا هي كما يلي: (5 dB- 10 dB) يعتبر أقل من المستوى الأدنى لتأسيس اتصال ، بينما (10 dB- 15 dB) هو الحد الأدنى المقبول لإنشاء اتصال غير موثوق ، (15 dB- 25 dB) هو المستوى الأدنى لإنشاء اتصال بطريقة مقبولة ، تعتبر (25 dB- 40 dB) نسبة جيدة جدًا لاستكمال الاتصال ، ومن 41 dB وما فوق تعتبر ممتازة.

أخيرًا ، باستخدام كل من مصفوفات القناة التحليلية والمادية ، منحنيات MSE مقابل SNR لـ MIMO-OFDM. تتم مقارنة القيم النظرية للمشكلات الصغيرة بنتائج المحاكاة الحاسوبية. تناسب منحنيات المحاكاة النظرية والحاسوبية بشكل جيد للغاية ، خاصة عند مستويات SNR العالية.

نظام بصري باستخدام ثنائيات ليزريه وجهاز استقبال تنوع الزاويه

MIMO-OFDM

الاطروحـــة

مقدمـة الى قسـم هندسـة تقنيـات الاتصـالات كجزء من متطلبــات نيل درجة

المــاجستير

تقدمت بـها

هاله كاظم محمد

اشــراف

الدكتـور نـاصر حسين سلمان

2021

جمهوريــة العراق
وزارة التعليم العــالي والبـحث العلـمي
جــامعة الفــرات الاوسط الـتقنية
الكلية التقنية الـهندسية- نجف

نظام بصري باستخدام ثنائيات ليزريه وجهاز استقبال تنوع الزاوية MIMO-OFDM

هاله كاظم محمد

بكالوريوس في هندسة تقنيات الاتصالات

2021